Biosensors and Bioelectronics 89 (2017) 107–122

Contents lists available at ScienceDirect

Biosensors and Bioelectronics

journal homepage: www.elsevier.com/locate/bios

Graphene-based screen-printed electrochemical (bio)sensors and their applications: Efforts and criticisms

Stefano Cinti [a,b], Fabiana Arduini [a,b,*]

[a] Department of Chemical Sciences and Technologies, University of Rome "Tor Vergata", Via della Ricerca Scientifica, 00133 Rome, Italy
[b] National Institute of Biostructures and Biosystems, Viale delle Medaglie d'Oro 305, 00136 Rome, Italy

ARTICLE INFO

Article history:
Received 1 December 2015
Received in revised form
22 June 2016
Accepted 3 July 2016
Available online 5 July 2016

Keywords:
Graphene
Electrochemical biosensor
Electrochemical sensor
Screen-printed electrode

ABSTRACT

K.S. Novoselov in his Nobel lecture (December 8, 2010), described graphene as "*more than just a flat crystal*" and summarized the best possible impression of graphene with *(i) it is the first example of 2D atomic crystals, (ii) it demonstrated unique electronic properties, thanks to charge carriers which mimic massless relativistic particles, and (iii) it has promise for a number of applications.* The fascinating and unusual properties of this 2D material were indeed recently investigated and exploited in several disciplines including physics, medicine, and chemistry, indicating the extremely versatile and polyedric aspect of this nanomaterial.

The utilization of nanomaterials, printed technology, and microfluidics in electroanalysis has resulted in a period that can be called the "Electroanalysis Renaissance" (Escarpa, 2012) in which graphene is without any doubt a forefront nanomaterial. The rise in affordable fabrication processes, along with the great dispersing attitude in a plenty of matrices, have made graphene powerful in large-scale production of electrochemical platforms. Herein, we overview the employment of graphene to customize and/or fabricate printable based (bio)sensors over the past 5 years, including several modification approaches such as drop casting, screen- and inkjet-printing, different strategies of graphene-based sensing, and applications as well. The objective of this review is to provide a critical perspective related to advantages and disadvantages of using graphene in biosensing tools, based on screen-printed sensors.

Contents

* Corresponding author at: Dipartimento di Scienze e Tecnologie Chimiche, Università Roma Tor Vergata, Via della Ricerca Scientifica, 00133 Rome, Italy.
E-mail address: fabiana.arduini@uniroma2.it (F. Arduini).

http://dx.doi.org/10.1016/j.bios.2016.07.005
0956-5663/

1. Introduction

Andre K. Geim and Konstantin S. Novoselov described in their article (Novoselov et al., 2004) the remarkable observation of the electric field effect in thick monocrystalline graphitic film: the film remains metallic, continuous and of high quality down to a few atomic layers. Graphene, obtained from pyrolytic graphite by an easy exfoliation technique, was the name given to those single layers of carbon atoms. These 2D sheets, in which carbon atoms are covalently bonded into a sp^2-atom network, reveal them as a cornucopia of new physics, leading to plenty of potential innovative applications (Geim and Novoselov, 2007).

Graphene possesses extraordinary properties, such as large surface area, thermal conductivity, charge carrier mobility, and mechanical strength, respectively measured equal to above 2600 $m^2 g^{-1}$layer^{-1}, 3000 W mK^{-1}, 10,000 $cm^2 V^{-1} s^{-1}$, and 1 TPa (Stankovich et al., 2006; Balandin, 2011; Mayorov et al., 2011; Lee et al., 2008; Geim and Novoselov, 2007).

Chosen for its outstanding properties, graphene has potential, attractive applications in many fields such as solar cells (Wang et al., 2008), photonics (Bonaccorso et al., 2010), energy storage (Yang et al., 2010), GHz transistors (Lin et al., 2010), and nanoelectronics (Eda et al., 2008). Regardless of these scenarios, the production of graphene represents a real challenge nowadays (Avouris and Dimitrakopoulos, 2012; Torres and Kaner, 2014). Depending on the specific application, there are several methods to mass-produce graphene, which allows for a wide range of graphene size, quality, and price (Novoselov et al., 2012). Mechanical and chemical graphite exfoliation (Dreyer et al., 2010), epitaxial growth on silicon carbide (Virojanadara et al., 2008), chemical vapor deposition (CVD) (Obraztov, 2009), and "unzipping" of carbon nanotubes (CNTs) (Kosynkin et al., 2009) represent just some of the dozen methods developed to obtain graphene. In spite of the discovery of graphene sheet achieved by a mechanical cleavage, the low productivity of this approach makes it unsuitable for large-scale use. Chemically-exfoliated graphite and chemical reduction of exfoliated graphite oxide allow for an efficient and cost effective production of bulky graphene sheets (McAllister et al., 2007; Stankovich et al., 2007). A powerful feature of graphene is seen in its flexibility for the creation of dispersions and nanocomposites. However, when discussing on "graphene", the terminology should be addressed very carefully. Depending on the number of layers (single, few, multi) and the carbon source (graphite, CNTs), it is possible to obtain various form of chemically modified graphene, including graphene oxide (GO), reduced graphene oxide (rGO) or graphene nanoribbons (GNRs) after unzipping the CNTs. With respect to considered material, many differences could be observed (Martin and Escarpa, 2014). Due to its ease of synthesis and satisfying dispersion processability, graphene becomes inexpensive and attractive for mass-scale applications in a conventional technological field, such as the development of electrochemical devices (Li et al., 2008a). However, large-scale and low-cost production of electrochemical devices is not attributable just to graphene or other innovative materials. Concerning electrochemical (bio)sensors, a critical role towards cost lowering is certainly attributable to the electrodes utilized. Economic criteria should not, in any case, reduce the reproducibility and sensitivity of the detection methods towards target analytes. Furthermore, it is also necessary to take into account the time consumption involved in the production/modification/treatment of electrodes. Printing technology has appeared, in the last twenty years, as the most favorable methodology for the high-volume serial production of reliable single-use devices, keeping high both their affordability and analytical performance. Printed technology has contributed tremendously in the development of point-of-care (POC) devices. Taken from an IDTechEx report entitled "Printed and Flexible Sensors 2015–2025: Technologies, Players, Forecasts" released in 2015, the market of printed, flexible, and organic electronics is rapidly growing and will be worth more than $60 billion by 2025 (Das and Harrop, 2013).

Customization of conductive inks, substrates, and patterns, has made screen-printed electrodes (SPEs) a versatile tool in accordance with the analytical requests, particularly thanks to their suitability to be modified. SPEs can be modified by incorporating enzymes, nucleic acids, metals, polymers, or electrochemical mediators, directly in the ink or subsequently by using drop-castable dispersions, as reported in a wide number of reviews (Metters et al., 2011; Li et al., 2012; Windmiller and Wang, 2013; Taleat et al., 2014; Thiyagarajan et al., 2014; Arduini et al., 2016). Graphene represents one of the most used materials as electrode modifier, thanks to its excellent properties in dramatically enhancing the performance of various electroanalytical systems (Lawal, 2015).

This review will to provide a comprehensive overview focused on the employment of graphene and graphene-based composites in screen-printed electrochemical sensors and biosensors. The latest developments regarding SPEs modified by means of this two-dimensional material, will be critically discussed in order to rationalize which are the advantages and drawbacks, in terms of electrocatalysis, sensitivity, inorganic and biomolecular loading, and costs for electrochemical (bio)sensor development.

2. Fabrication of graphene-based screen-printed electrodes

Depending on the specific need and economic opportunities/facilities, different strategies exist nowadays with respect to the manufacturing and modification of printed electrodes (Albareda-Sirvent et al., 2000; Laschi and Mascini, 2006; Dominguez Renedo et al., 2007; Singh et al., 2010). The widely adopted fabrication of printed sensors is based on thick-film technology, with the production of SPEs being the most used printed sensors reported in literature. The peculiarity of disposable SPEs is observed by the enormous possibility for mass utilization, allowing easy customization, coupled with effective portability, cost-effectiveness, and considerable application directly on field (Metters et al., 2011). Graphene has been involved in this kind of customization because of its prominent electrochemistry (Brownson et al., 2012).

2.1. Screen-printed electrodes modified with graphene by drop casting

The most widely used approach to modify SPEs, over the large-scale, is certainly represented by drop casting of graphene dispersion over an underlying substrate. Depending on production methods and chemical functionalizations, graphene can be obtained as dispersion by utilizing various solvents (e.g. water, ethanol, acetone, hexane, dimethylformamide (Paredes et al., 2008)). This method

facilitates the study of the effect of the dispersion composition on the detection capabilities, tailoring analytical features like sensitivity, detection limit, and reproducibility. Additionally, the study requires small amount of dispersible material. Cysteine-GO, easily dispersed in water, has been drop-cast onto SPE, producing with gold nanorods a 3D-layered gold nanorods-containing structure. These modified SPEs showed a better electrochemical performance with respect to the unmodified ones. Because of its high surface area, graphene allowed to minimize the formation of electrochemically poor catalyst-aggregates towards hydrogen peroxide detection (Xue et al., 2015). Graphene offers many possibilities in the choice of dispersing media, depending on the task it should accomplish. By dispersing graphene into poly(sodium 4-styrenesulfonate) (PSS), drop cast SPEs highlighted an increase of sensitivity towards detection of heavy metals (Huangfu et al., 2013). Even the biocompatible chitosan has been used as dispersing media to enhance the film formation of graphene onto SPE (Apetrei et al., 2016). Sometimes, as in the case of the nanocomposite formed by platinum, copper oxide, and rGO, an organic solvent such as dimethylformamide has been needed to obtain a satisfying dispersion (Dhara et al., 2014). SPEs have been quickly drop cast without any ink-related issues. Yet, particularly in laboratory-scale processes, this approach could be characterized by some drawbacks as the low homogeneity of the resulted modified-surface. A phenomena known as “coffee ring” effect was observed, due to capillary forces present as a result of solvent evaporation which can push the modifier, e.g. graphene, platelets to the edges of the underlying electrode (Deegan et al., 1997). These devices may lack in reproducibility due to graphene agglomeration. However, the issue related to this feature can be easily addressed by using automatic dispensing system as Biodot(R) (www.biodot.com), by means of a spray deposition (Gilje et al., 2007) or by using more sophisticated instrumentations such as an inkjet printer, which allows for the deposition of picolitre drops (Calvert, 2001).

2.2. *Screen-printed electrodes modified with graphene by ink-printing*

Inkjet-printing has been largely utilized as a SPE-modifying approach, by using graphene as well as a variety of nanomaterials. The advantages rely on most controllable dispersion deposition because inkjetted drops rapidly evaporate. Tuantranont’s group has reported on the use of a Fujifilm Dimatix inkjet-printer, to rapidly modify SPEs by-means of a graphene-poly (3,4-ethylenedioxythiophene): poly(styrene-sulfonate) (GR-PEDOT:PSS) dispersion. Many analytes have been detected with modified-SPEs, obtaining satisfactory reproducibility with the opportunity to rationally tune the performance modulating the number of printed graphene layers (Karuwan et al., 2012; Sriprachuabwong et al., 2012).

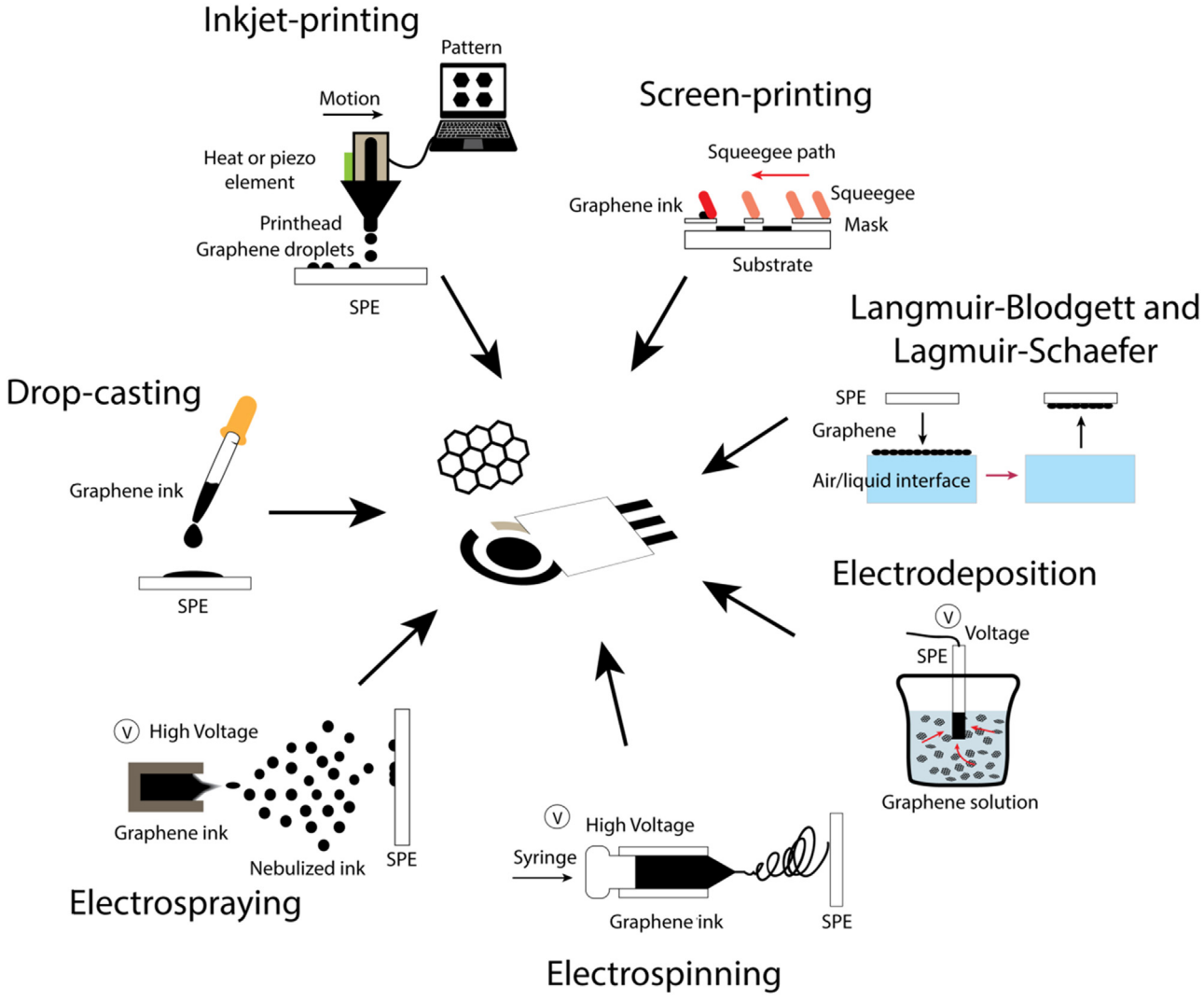

Fig. 1. Scheme of the several procedures utilized for fabrication of SPEs modified with graphene.

2.3. Graphene based screen-printed electrode production using graphene-ink

Another approach for graphene-SPE production, is thick-film technology using ink modified with graphene, since graphene can be easily incorporated into the conductive-ink (often graphite-based). Currently, many reputable manufacturing companies are leading the large-scale market of inks and SPEs, such as DropSens, Zensor, Kanichi, Gwent (www.dropsens.com; www.zensor.com.tw; www.kanichi-research.com; www.gwent.org). SPE modified with graphene (GR-SPE) manufactured by DropSens, code: DRP-110GPH, is one of the most literature-reported commercialized SPE, finding applications in several fields (Eissa and Zoroub, 2012; Antiochia and Gorton, 2014; Guiberteau-Cabanillas et al., 2015). Commercially available printable graphene inks (Randviir et al., 2014), or lab-synthesized powder mixed into conductive ink (Ping et al., 2012a), can be used to produce lab-made GR-SPE. Yet, even if screen-printing represents nowadays one of the most promising technologies, particularly towards miniaturization, the plausibility of this approach reflects in some drawbacks too. Rheological properties of the inks should be taken into account: viscosity represents the major limitation in modifying the ink with a powder.

2.4. Screen-printed electrodes modified with graphene by electrodeposition

On the other hand, SPEs can be easily modified by electrodepositing graphene on the surface of the working electrode. Many works have been reported on the use of this kind of approach, utilizing a plenty of different graphene-containing mixtures. Typically, SPEs are modified by cathodic amperometry or cyclic voltammetry, as widely reported in literature (Yang et al., 2013; Jian et al., 2013; Ping et al., 2014; Istrate et al., 2016). Electrochemical methodologies represent an accurate method to modify the electrode surface, such as control of the film thickness, but they contain intrinsic limitations that make it difficult to extend them to a large-scale production.

2.5. Other methods

In addition to these four mainly adopted approaches, other manufacturing strategies have been employed. Langmuir-Blodgett (LB) can be utilized to manufacture an organized layer of graphene onto a vertical substrate (Li et al., 2008b). Langmuir-Schaefer (LS) is another approach in which the deposition is done by dipping the substrate horizontally, in contact with the monolayer as reported by Michopoulos et al. (2014) who modified SPE with a film containing GO-Prussian Blue (PB) hybrid nanocomposite. The recently innovative method for SPE modification with graphene involved electrospray deposition. Graphene has been efficiently electrosprayed onto SPE by means of a custom-built system as reported by Henry's group (Ruecha et al., 2015), demonstrating a low-cost alternative solution to more often-used methodologies. Electrospinning is also a recent technique employed for SPE modification. In this process, a polymer solution is injected from a needle in the presence of an electric field (Greiner and Wendorff, 2007). This is a simple and cost-effective technique, as demonstrated by Promphet et al. (2015) who electrospun a composite made by graphene, polyaniline and polystyrene to detect heavy metals. The main drawback of this approach is the necessity of a polymer matrix.

However, the suitability to modify SPEs with graphene offers a wide range of possibilities, and this paragraph includes the mainly adopted modification procedures schematized in Fig. 1. There is not a “right” method to incorporate graphene into a screen-printed electrode, but the chosen approach depends solely on the analytical requirements and on the economical possibilities.

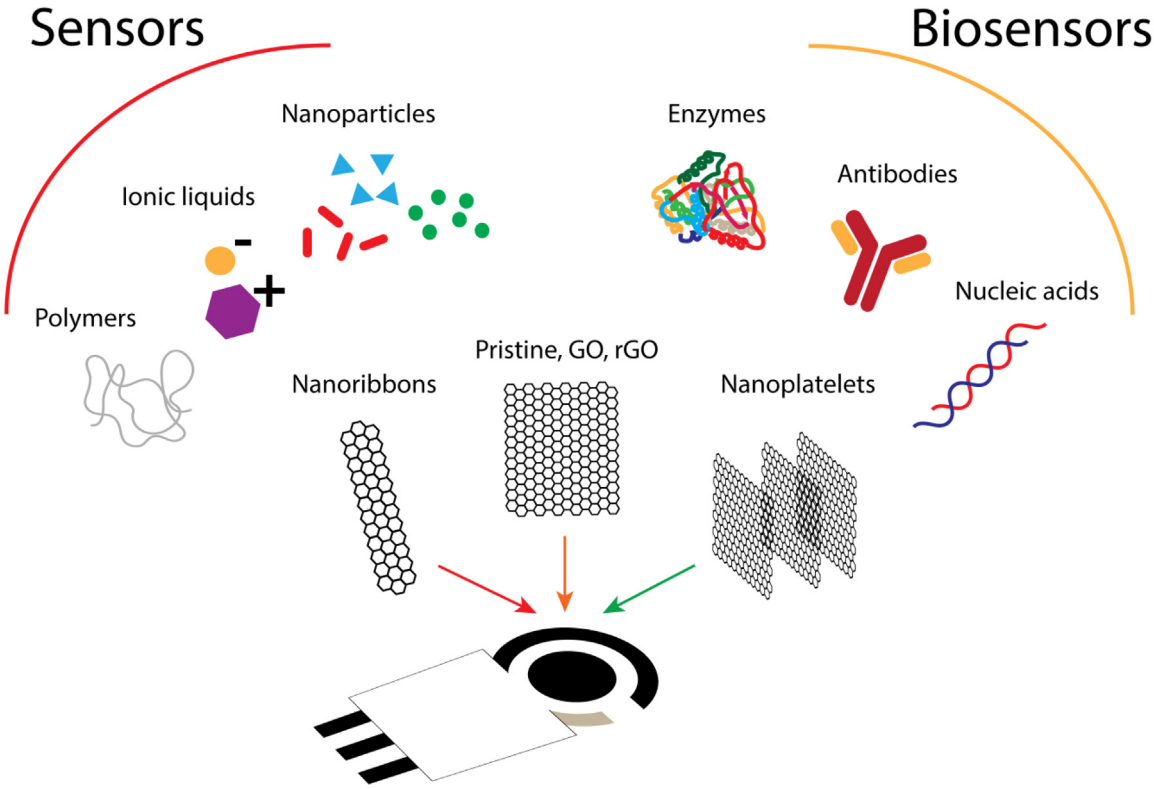

Fig. 2. Scheme of the different graphene-based screen-printed electrochemical (bio)sensors.

3. Biosensors based on graphene and screen-printed electrodes

According to the technical report published on *Biosensors and Bioelectronic* in 2001, an electrochemical biosensor is defined as a self integrated device capable of providing quantitative or semi-quantitative analytical information using biological recognition element (biochemical receptor like enzyme, DNA sequence, and antibody) in direct spatial contact with the electrochemical transduction element. Biosensors may be classified according to the biological specificity-conferring mechanism or, alternatively, to the mode of physio-chemical signal transduction (Thevenot et al., 2001) Since this review focused on electrochemical transduction using SPEs, the classification of biosensors were made as a function of biocomponent immobilized onto the surface of the working electrode, including enzymatic biosensors, immunosensors, and DNA sensors (Fig. 2).

3.1. Enzymatic biosensors

Glucose biosensors based on the use of glucose oxidase are, without any doubt, the most studied enzymatic biosensors, beginning with the first biosensor designed by Updike and Hicks (1967), to the first pen-sized biosensor launched in market by Medisense Inc. (1987) for self-monitoring of blood glucose by diabetic patients, and arriving at the recent innovative biosensors based on SPEs modified with graphene. The importance of the glucose biosensor is related to the necessity of glucose self-monitoring by diabetic patients, and taking into account that this disease affects roughly 150 M people worldwide (Wang, 2008; Privett et al., 2008; Zhu et al., 2012; Scognamiglio, 2013). Daily, millions of diabetics test their glycemic levels by using commercial biosensor strips. 85% of the entire biosensor market is hosted by glucose biosensors (Turner, 2013).

The detection of glucose using GR-SPEs was focused on the detection of enzymatic product as well as direct electron transfer of glucose oxidase.

To our knowledge, the first glucose biosensor employing graphene and a SPE was reported in 2011 (Ping et al., 2011). Ping and coworkers deposited rGO by one-step electrodeposition of the exfoliated GO sheets onto the ionic liquid doped SPE. The modified electrode has demonstrated the ability to detect hydrogen peroxide (enzymatic product) at negative applied potential (−0.2 V vs Ag/AgCl) with a linear range comprised from 0.15 μM to 1.8 mM. This sensor was then used as platform to develop a glucose biosensor by immobilising the glucose oxidase by using a cross-linking method using glutaraldehyde. The glucose was detected with sensitivity of 22.78 $\mu A\, mM^{-1}\, cm^{-2}$, linear range up to 10 mM, and detection limit of 1.0 μM. The suitability of the biosensor was challenged in milk samples with satisfactory recovery values, indicating the potential application of this biosensor for determination of glucose in a real sample.

The detection of glucose by direct electron transfer of glucose oxidase was reported by Wisitsoraat et al. (2013) and Chia et al.

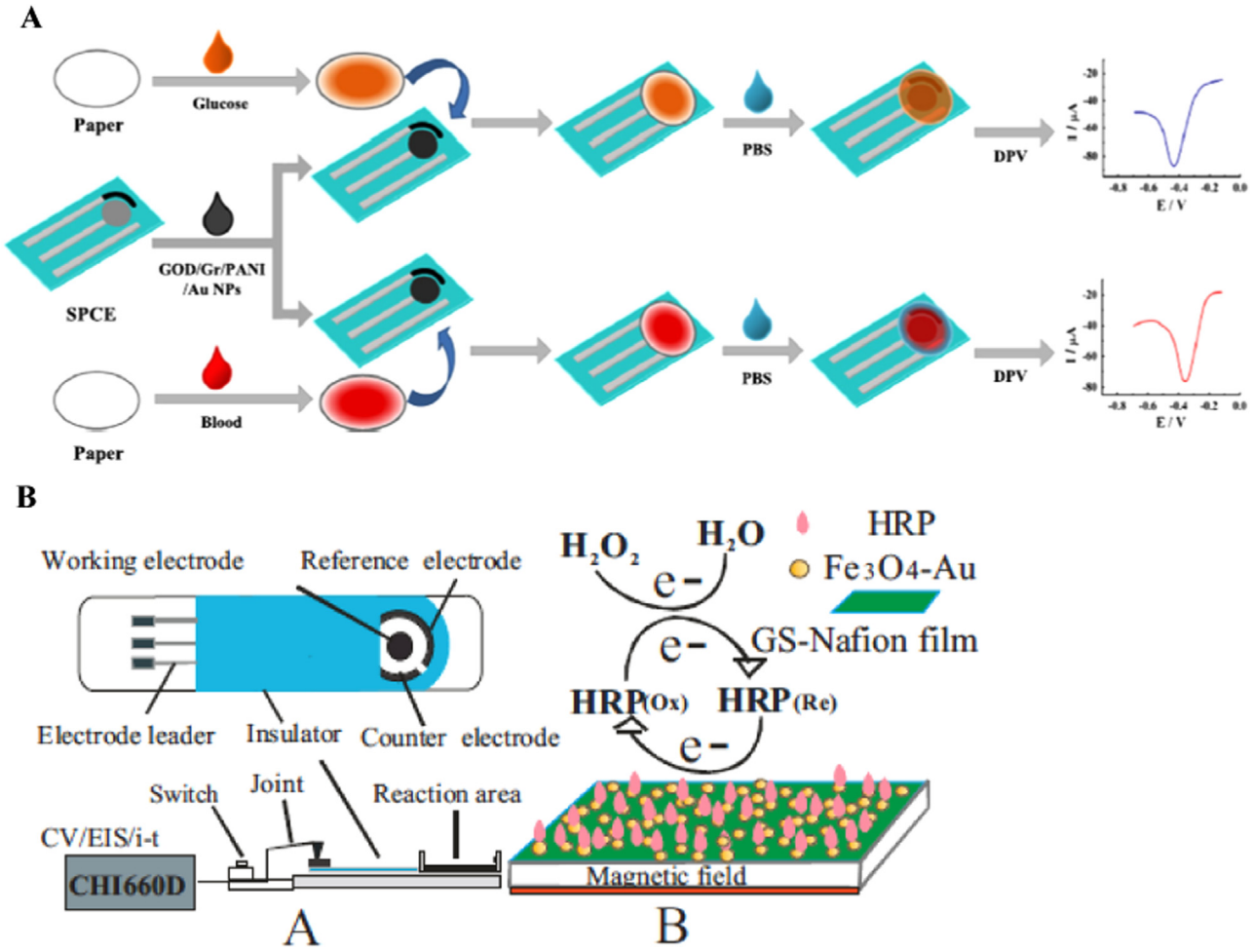

Fig. 3. Schematic representation of: (A) paper-based *enzymatic* glucose sensor device using glucose oxidase immobilised onto graphene modified SPE and a paper disk for sample loading (Kong et al., 2014); (B) disposable *enzymatic* biosensor for hydrogen peroxide determination using GR-SPE and Fe_3O_4–Au magnetic nanoparticles coated with horseradish peroxidase (Xin et al., 2013). Reprinted with permission from Ref. (Kong et al., 2014; Xin et al., 2013).

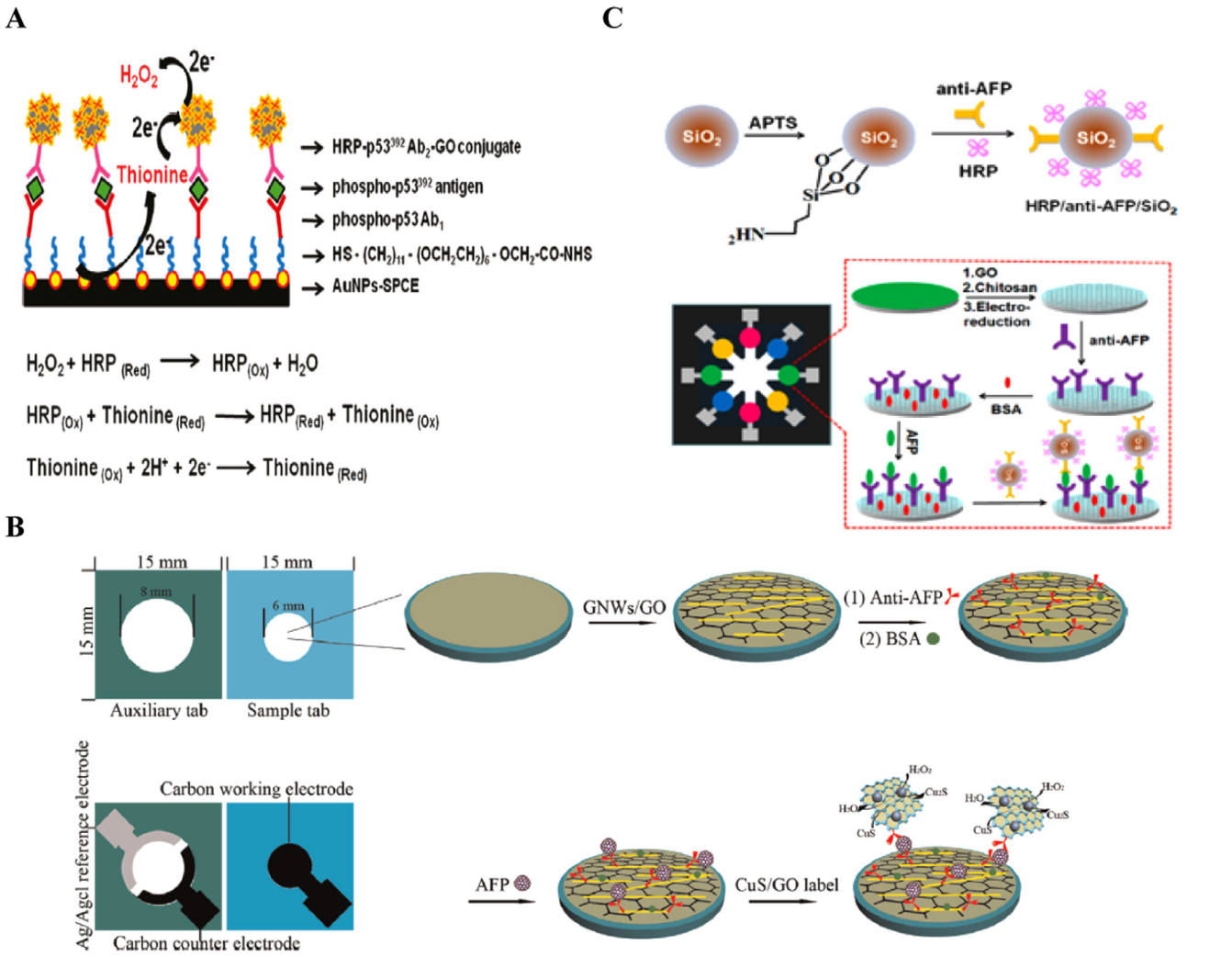

Fig. 4. Schematic representation of: (A) *immunosensor* for p53 (Ser 392) protein detection using a novel nanocomposite based on GO as support for HRP enzyme and antibody (p53^{392}Ab$_2$) immobilization. The sandwich format was designed by immobilizing primary antibody (p53^{392}Ab$_1$) on the SPE and quantifying the binding antigen/antibody with the nanocomposite (Du et al., 2011); (B) *immunosensor* for α-fetoprotein measurement designed by immobilizing the capture antibody onto the working electrode surface, previously modified by drop casting GO and ultrathin gold nanowires. The binding with α-fetoprotein was evaluated by adding CuS nanoparticle-decorated graphene (CuS/GO) composites labeled with signal antibodies (Li et al., 2015); (C) *immunosensors* for multiplexed analysis of four cancer biomarkers namely, alpha-fetoprotein (AFP), carcinoembryonic antigen (CEA), cancer antigen 125 (CA125), and carbohydrate antigen 153 (CA153) using μPED and graphene. These immunosensors included the immobilization of capture antibodies onto the working electrode surfaces modified with GO by drop casting, and the use of the antibody and HRP coimmobilized on SiO_2 manoparticles for signal out-put (Wu et al., 2013). Reprinted with permission from Ref. (Du et al., 2011; Li et al., 2015; Wu et al., 2013).

(2015). In the first case, graphene–poly(3,4-ethylenedioxythiophene): polystyrene sulfonic was modified on a SPE, and was used with immobilized glucose oxidase via glutaraldehyde. The detection of glucose was performed by direct electrochemistry of glucose oxidase at a −0.4 V applied potential, displaying a sensitivity of 7.23 μA mM^{-1} with a detection limit of 0.3 μM. In the second case, a SPE was modified with graphene produced by a novel and green method via mild sono-chemical alcohol–water treatment. The glucose enzyme was immobilized by exploiting the succinimidyl ester moiety of pyrenebutyric acid N-hydroxysuccinimide added in graphene dispersion. The biosensor was embedded in a flow system with applied potential of −0.4 V, observing sensitivity of 32.15 μA mM^{-1} cm^{-2} and detection limit of 28.3 μM.

Recently, the WHO has established the guidelines for ASSURED devices, which must be affordable, sensitive, specific, user-friendly, rapid and robust, equipment-free, deliverable. These requirements have shifted recent research activity towards paper based electrochemical biosensors. Paper based microfluidic devices (μPED) coupled the feasibility of the printed sensors with the advantages of paper, including a sustainable substrate material and flow analysis without the need of a pump. In this contest, an interesting biosensor based on the use of GR-SPE with a paper disk was reported by Kong et al. (2014). Biocomposite, prepared using graphene/polyaniline/gold nanoparticles and glucose oxidase, was used to modify a SPE. After that, the glucose standard dilution or blood sample was loaded onto the paper disk, which laminated onto the electrode strip to fully cover the three-electrode configuration. For glucose measurements only some μL of buffer was dropped on the paper disk (Fig. 3A). The innovative biosensor was enabled to quantitatively measure glucose from 0.2 mM up to 11.2 mM, with a detection limit of 0.1 mM, and it was successfully applied in a whole blood sample. Additionally, other enzymes have been used for biosensor development. Horseradish peroxidase enzyme was immobilised on Fe_3O_4–Au magnetic nanoparticles, and hydrogen peroxide was detected exploiting the direct electron transfer of horseradish peroxidase with linear range up to 2.5 mM and detection limit of 12 μM (Fig. 3B). However, the measurement needed to be carried out under N_2 protection, limiting the application in field (Xin et al., 2013).

A commercial graphene based SPE was developed for fructose detection, immobilizing fructose dehydrogenase enzyme and osmium-polymer. The osmium-polymer is able to work as an electrochemical mediator, as well as support for direct wiring of bound cofactor flavin adenine dinucleotide onto the electrode surface. The biosensor has reported good linear range and a low detection limit equal to 0.8 μM. The authors highlighted the better analytical features achieved than those obtained with similar biosensors based on Os-polymer modified screen-printed SWCNT and MWCNT electrodes (Antiochia and Gorton, 2014).

3.2. Immunosensors

One research activity line carried out in the last years for immunosensor development was focused on cancer biomarker detection. The use of graphene has been tried extensively in this sector, embracing different aspects of cancer management. Graphene, in the immunosensor field, was used to improve the electrochemical performances of SPEs, as in the enzymatic biosensor, and/or also to load antibodies and enzymes for signal output enhancement.

The properties to load effectively, even higher than other nanocarriers demonstrated in drug delivery (Sun et al., 2008), were recently exploited in the sensing area as well. Du et al. (2011) have reported an immunosensor for p53 (Ser 392) protein detection, a tumor suppressor and transcription factor, using a novel nanocomposite based on GO as support for HRP enzyme and antibody ($p^{53392}Ab_2$) immobilization. The sandwich format was designed by immobilizing primary antibody ($p53^{392}Ab_1$) on the SPE and quantifying the binding antigen/antibody with the previously prepared nanocomposite (Fig. 4A). Using this immunosensor, a linear response over the concentration range from 0.02 to 2 nM was obtained with the detection limit of 0.01 nM. The authors highlighted that the detection limit achieved is 10-fold lower than that of a conventional sensor with the HRP-streptavidin-biotin-$p53^{392}Ab_2$. The effectiveness of this novel immunosensor was tested against human plasma spiked with phospho-$p53^{392}$, demonstrating good accuracy. In the aforementioned work, graphene was employed to load antibody and enzyme for signal output, graphene was also used as a material to improve the measurement in the label free immunosensor. Teixeira and coworkers have developed a label free immunosensor for human chorionic gonadotropin (hCG) detection using electrochemical impedance spectroscopy and commercially available GR-SPE. In this case, graphene was used as an SPE working electrode modifier (Teixeira et al., 2014). In detail, the GR-SPE was modified with an amine layer, obtained with in situ electropolymerization of aniline, for the reaction with the carboxylic groups of the antibody, activated by carbodiimide chemistry to ensure successful antibody binding. The label free detection is achieved thanks to the electrochemical impedance spectroscopy technique that is able to quantify the resistance of charge transfer, and the biomolecule loaded onto working electrode surface (Prodromidis, 2010; Arduini et al., 2015). This immunosensor has detected hCG in urine with linear behavior from 0.001 to 50 ng mL^{-1} in less 20 min, demonstrating the utility of this immunosensor taking into account that hCG is also considered a specific marker for trophoblastic tumors of placental and germ cell origin (Stenman et al., 2004). Graphene was also employed with carbon nanotubes to measure miRNAs, which are promising candidates for different tumor assessments, as well as to predict their clinical behavior (Visone and Croce, 2009). The gold SPE was modified by drop casting RGO and MWCNTs, and then oligonucleotide capture probes were grafted and complementary miRNA was added. An antibody directed to RNA was employed along with a secondary antibody conjugated to HRP for hybridization assessment. This complex architecture allows the quantification of mRi-141 with detection limit down to 10 fM (Tran et al., 2014). The development of an attractive μPED, aforementioned in the enzymatic biosensor section, was also observed in immunosensor development using chromatographic paper or vegetable parchment as substrates (Wu et al., 2013; Yan et al., 2012).

Li et al. (2015) have developed an innovative immunosensor for the tumor marker α-fetoprotein. The immunoassay was designed by immobilizing the capture antibody onto the working electrode surface, previously modified by drop casting GO and ultrathin gold nanowires. The binding with α-fetoprotein was evaluated by adding CuS nanoparticle-decorated graphene (CuS/GO) composites labeled with signal antibodies (Fig. 4B). The CuS/GO nanocomposite was employed since it possesses efficient electrocatalytic activity toward the reduction of H_2O_2. This immunosensor enabled α-fetoprotein (AFP) measurement as low as 0.5 pg mL^{-1}, and it was successfully applied for AFP quantification in serum sample of healthy people as well as cancer patients. In this work, the graphene demonstrated the capability to improve the electrochemical performances of the SPE, and antibody loading as well.

A multiplexed analysis using μPED and graphene was reported for the first time by Wu and coworkers for detection of four cancer biomarkers namely, AFP, carcinoembryonic antigen (CEA), cancer antigen 125 (CA125), and carbohydrate antigen 153 (CA153) (Wu et al., 2013). These immunosensors included the immobilization of capture antibodies onto the working electrode surfaces modified with GO by drop casting, and the use of the antibody and HRP coimmobilized on SiO_2 manoparticles for signal out-put (Fig. 4C). The lowest detectable concentrations for AFP, CEA, CA125, and CA153 were 0.001, 0.005, 0.001, and 0.005 ng mL^{-1}, respectively. The authors highlighted the high sensitivity of these immunosensors thanks to i) the presence of graphene onto the surface able to efficiently accelerate the electron transfer and ii) the use of large silica nanoparticles as a label to reduce the physical adsorption.

Immunosensors were also developed for applications in the pharmaceutical and agri-food sectors.

CEA was also detected with a sandwich-type electrochemical immunosensor using SPE modified with reduced graphene oxide and silver nanoparticles, primary (capture) antibody immobilised onto working electrode and horseradish peroxidase (HRP)-conjugated secondary (detection) antibody. This immunosensor was capable to quantify CEA with a detection limit down to 0.035 μg mL^{-1} (Lee et al., 2016).

The Zharoub's group has developed a label-free voltammetric immunosensor for the sensitive detection of β-lactoglobulin and okadaic acid using a simple and efficient electrografting method to functionalize graphene modified SPE. This method involved the electrochemical reduction of in situ generated 4-carboxyphenyl diazonium salt in acidic aqueous solution to functionalize graphene (Eissa et al., 2012; Eissa and Zoroub, 2012). The label free sensing was achieved by analyzing the differential pulse voltammetry response of the ferro/ferricyanide redox probe; indeed a linear decrease was observed with increase of β-lactoglobulin concentration due to the formation of antibody–antigen complex onto the working electrode surface. The detection limit was 0.85 ng L^{-1} and 19 ng L^{-1} for β-lactoglobulin and okadaic acid, respectively. These immunosensors were successfully applied to real samples such as commercial milk-containing food products, in the case of β-lactoglobulin (Eissa et al., 2012). In the case of applications in pharmaceutical field, an immunosensor was developed for clenbuterol, a β-agonizts used orally in asthma treatment. The format is almost similar with the one reported in Fig. 3B where instead of enzyme, the antibody was immobilised on Fe_3O_4-Au magnetic nanoparticles, and the analyte was quantified using a

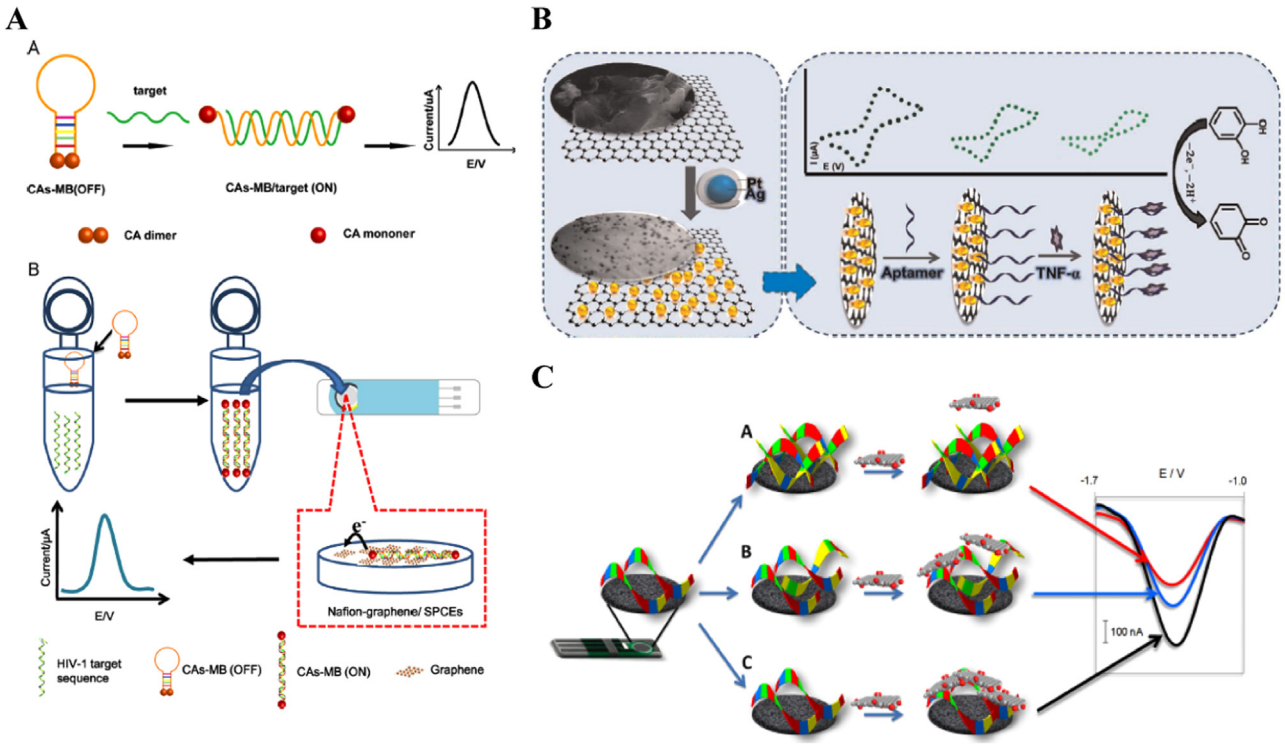

Fig. 5. Schematic representation of: (A) *DNA sensor* based on electrochemical molecular beacon sensing assay for HIV-oligonucleotide showing (A) Hybridization of electrochemically active–inactive switching molecular beacon with the HIV target oligonucleotide and (B) detection procedures (Li et al., 2014); (B) *DNA sensor* for protein TNF-α detection based on gold SPE modified with graphene oxide nanosheets loaded with bimetallic Ag@Pt core–shell nanoparticles. Determination of TNF-α was based on obstruction to the electrocatalytic oxidation of catechol by Ag@PtGRs after binding to the surface of the electrode through interaction with the aptamer (Mazloum-Ardakani et al., 2015); (C) *DNA sensor* based on inherently electroactive property of GO nanoplates, exploiting the different binding ability of single-stranded and double-stranded DNA towards GO nanoplatelets. The scheme reports the hybridization step with complementary target (A); one-mismatch target (B); and noncomplementary target (C) (Bonanni et al., 2012). Reprinted with permission from Ref. (Li et al., 2014; Mazloum-Ardakani et al., 2015; Bonanni et al., 2012).

competitive immunoassay. The binding between antibody and antigen was measured by monitoring the response of the differential pulse voltammetry reduction peak of ferro/ferricyanide redox probe (Yang et al., 2014). Recently, SPE modified with graphene sheets and gold nanoparticles was exploited to produce an electrochemical sandwich immunoassay for the human epididymis-specific protein 4 (HE4) detection. This immunosensor was based on the use of biotinylated monoclonal antibody against HE4 (anti-HE4) bound to streptavidin-modified magnetic beads via biotin-avidin. The immunocomplex was monitored using horseradish peroxidase (HRP)-labeled HE4 antibody. A commercially available electromagnetic detector device coupled with SPE allowing the HE4 detection up to 400 pM with a detection limit of 0.5 pM (Lu et al., 2016).

3.3. DNA sensors

The use of graphene and DNA has emerged in the biosensor field because it allows for several innovative sensing strategies. Regarding DNA sensor development, graphene was used as a modifier for the working electrode surface as well as a loading agent. For instance, sensitive determination of HIV-1 was carried out using an electrochemical molecular beacon, based on an active–inactive switch, combined with a nafion–graphene composite film modified SPE (Li et al., 2014). As schematized in Fig. 5A in the absence of the HIV-1 gag gene oligonucleotide, CA monomers were close enough to form a CA dimer in both ends of the molecular beacon with a stem–loop structure, thus the electrochemical signal was switched off. However, in the presence of HIV-1 gag gene oligonucleotide, the CA dimer was subjected to conformational change and the electrochemical signal was switched on. The response toward the target oligonucleotide resulted linear in a logarithmic scale from 40 nM to 2.56 μM, with a detection limit of 5 nM. The authors highlighted the improvement of using a SPE modified with graphene, with respect to bare SPE, with the current signal of free CA using GR-SPE at least six times higher than bare SPE.

The improvement of electrochemical behavior with a modified gold SPE, modified with graphene oxide nanosheets loaded with bimetallic Ag@Pt core–shell nanoparticles, was reported by Mazloum-Ardakani and coworkers for protein biomarker tumor necrosis factor-alpha (TNF-α) detection (Mazloum-Ardakani et al., 2015). Determination of TNF-α antigen was based on obstruction to the electrocatalytic oxidation of catechol by Ag@PtGRs after binding to the surface of the electrode through interaction with the aptamer (Fig. 5B). The aptasensor detected TNF-α at up to 60 pg mL^{-1}, with a detection limit of 2.07 pg mL^{-1}, demonstrating its suitability also in serum samples. With respect to enzyme and immuno-based biosensors, a DNA sensor was also designed by exploiting the inherently electroactive property of GO nanoplatelets, as reported by Pumera and co-workers with an outstanding work (Bonanni et al., 2012). They developed a novel electrochemical sensing tool for single-nucleotide polymorphism detection based on interactions between graphene oxide nanoplatelets and DNA strands. The innovative electrochemical sensing tool was based on the different binding ability of single-stranded and double-stranded DNA towards GO nanoplatelets and the stronger ability of graphene to conjugate ssDNA with respect to dsDNA, demonstrating the inherently electroactive property of GO. In this way, the detection of a non-complementary target at SPE has yielded a higher voltammetric signal than the complementary target at a SPE as showed in Fig. 5C, because higher amounts of

graphene were confined on the working electrode surface in the case of ssDNA.

4. Electrochemical sensors

Graphene goes beyond biosensors. Its favorable properties make it a serious candidate in the development of electrode material in electroanalysis. Graphene and all its forms, comprising its nanocomposites, represent a building block towards the realization of bioelement-less platform. In the next section it will be shown a plethora of graphene-based electrochemical sensors developed to overcome many of the issues related to direct-electrochemistry sensing. As a direct competitor to CNTs, graphene tasks will be observed against small (bio)molecules detection. Graphene-based materials/devices for electroanalysis and electrocatalysis is worthy of discussion here.

4.1. Hydrogen peroxide (H_2O_2)

Hydrogen peroxide is one of the most important analytes to be detected, because of its presence in many enzymatic reactions (H_2O_2 is the product of several oxidases, e.g. glucose, cholesterol, and alcohol oxidase), and for its occurrence in food, pharmaceutical, clinical, industrial, and environmental analysis (Tsiafoulis et al., 2005; Carocho and Ferreira, 2013). Undoubtedly, electrochemical sensors have shown to be a consistent building block towards H_2O_2 detection because of their great versatility and cost-effectiveness (Chen et al., 2012). Nowadays, electrochemical rush is aimed by the necessity to discover/develop sensing elements that are able to detect H_2O_2 with the highest sensitivity and selectivity, while decreasing the oxidation/reduction overpotentials (Ricci and Palleschi, 2005; Shao et al., 2010; Chen et al., 2013). Among these, graphene has attracted considerable attention from both scientific and technological communities due to its *superior* electrocatalytic activity, and its effectiveness in hybrid composite development onto SPEs.

GNRs, originated from longitudinally unzipped CNTs, and doped with nitrogen to yield N-GNRs, highlighted greater sensitivity, selectivity, and stability towards H_2O_2 reduction (Shi et al., 2015). At a working potential of -0.4 V (vs. Ag/AgCl), N-GNRs-SPEs response were linear in the concentration ranges of 5–85 and 135–1285 μM, with a sensitivity of 2.18 and 0.64 mA cm^{-2} mM^{-1}, respectively, and a detection limit of 1.72 μM. An outstanding property of graphene is its capability to be assembled with very diverse materials reflecting a consequent variation of the analytical performances. Ping et al. (2011) reported on a sensitive H_2O_2 platform by electrochemically reducing (ER) exfoliated GO over a ionic liquid (IL)-cast SPE. In comparison with IL-SPE, ER-GO/IL-SPE displayed good linearity for the oxidation and reduction of H_2O_2 in the concentration ranges from 0.1 μM to 2.0 mM and from 0.15 μM to 1.8 mM, with detection limits equal to 0.05 and 0.08 μM, respectively. Electrocatalytic features of graphene have been also employed in combination with a conducting polymer matrix. Electrochemically exfoliated graphene has been dispersed in PEDOT:PSS and inkjetted onto SPEs (Sriprachuabwong et al., 2012). Presence of graphene has led to a signal approximately 13 and 3 times higher than that of bare and PEDOT:PSS-SPE, respectively. While graphene has provided effectively enhancements for SPEs, its intrinsic conductivity coupled with its great surface area and smoothness have been elegantly utilized for the best deposition of Prussian Blue (PB), *the* "artificial peroxidase" (Karyakin et al., 2000; Ricci and Palleschi, 2005). Michopoulos et al. (2014) have been functionalized a SPE with layer-by-layer approach involving octadecyl amine (ODA)-rGO-ODA-PB as modifiers. The reported configuration showed a linear response from 5 to 1000 μM H_2O_2, detection limit of 2 μM, and a repeatability lower than 5% (n = 10). As discussed, graphene in various forms has been able to enhance the detection of hydrogen peroxide with SPEs, both cathodically and anodically, through various (and easy) modification strategies.

4.2. Ascorbic acid (AA), uric acid (UA), and dopamine (DA)

Ascorbic acid (AA) is another electroactive analyte, which deserves to be detected because of its powerful antioxidant role (Smirnoff, 2000). Moreover, the oxidation of a neurotransmitter (and its precursors), such as dopamine (DA) or uric acid (UA), present with AA in biological tissues and liquids (serum, urine, saliva) occur at a potential close to that required as in the case of AA. Discrimination of these species is a very important requirement in order to avoid interferences, and GR-SPEs convincingly showed to accomplish this required task. Ping et al. (2012b) have developed a GR-SPE incorporating chemically rGO into the conductive ink. By cyclic voltammetry experiments, well-defined sharp and fully resolved anodic peaks were obtained, and very large peak potential separations were achieved: 221 mV for AA-DA, 173 mV for DA-UA, and 394 mV for UA-AA. Differential pulse voltammetry (DPV), allowed for the detection of AA, DA, and UA with detection limits evaluated as 0.95 μM, 0.12 μM, and 0.20 μM, respectively. These results have been critically discussed in a recent work of Banks' group (Randviir et al., 2014). They claimed that in the work reported by Ping et al. (2012b), the utilized graphene was fabricated through the chemical reduction of graphitic oxide, thus the reported 'electrocatalytic' effects resulted from a contribution from the presence of a large number of edge plane-like sites/defects present on the basal plane of the graphene surface and from metal ions. Randviir et al. utilized two different graphene-based inks, from different ink-companies, to screen-print electrodes, reporting on the fabrication of screen-printable graphene ink. Simultaneous detection of the three analytes (AA, DA, UA) was not always achieved, and the electrochemical properties of the GR-SPEs appeared diverse, in terms both of kinetics and analytical performances. GR was also used in combination with NiO for the simultaneous determination of DA and UA, observing a peak potential difference of 150 mV between DA and UA, and quantification of DA in the concentration range of 1.0–500.0 μM (Jahani and Beitollahi, 2016).

Recently, Martin et al. (2015) reported on the analytical performance of two GNR materials, oxidized GNR (GNRox) (high oxygen content $>40\%$ wt.) and reduced GNR (GNRred) (low oxygen content, $<20\%$ wt.), dispersed in a mixture water/NH_3 (1% v/v), and drop-cast onto SPE, towards detection of AA, levodopa (LD, precursor of DA), and UA. GNRred- and GNRox-SPE have been compared not only with the bare SPE, but also with other related carbon nanomaterials such as MWCNTs. Escarpa's group has demonstrated the excellent electrocatalysis exhibited by GNRred-SPEs by detecting AA, LD, and UA simultaneously at $+0.08$, $+0.27$, and $+0.39$ V, respectively. The authors ascribed these findings to the low percentage of oxygen moieties in the edge-plane capable of interacting differently with the analytes and discriminating the three different molecules. Step-by-step, it is becoming obvious how graphene synthesis, its composition "grade", and the approach of electrode modification, are able to *really* affect the analytical performance of such screen-printed platforms.

4.3. Glucose

The direct electro-oxidation of glucose without enzyme is an alternative route for glucose detection. Typically, metal-modified electrodes are used to carry out the enzyme-less detection of glucose, and graphene, due to its fabulous intrinsic properties, has

been reported as a very eclectic modifier in order to improve this detection. Yang et al. (2013) described the fabrication of a (chitosan)CS-rGO-(nickel nanoparticles)NiNPs-modified SPE by cathodic CV electrodeposition. rGO endowed hydrophobicity for deposition from the aqueous solution, helped the formation of CS-based nanocomposite scaffold to uniformly distributed NiNPs, reducing cluster formation, and provided fast electron transfer kinetics. CS-rGO-NiNPs-SPE exhibited outstanding performance for enzyme-less glucose sensing in alkaline media with high sensitivity, wide linear range, and low detection limit, respectively 318.4 $\mu A\ mM^{-1}\ cm^{-2}$, up to 9 mM, and 4.1 μM. Low-volume measurements of human urine samples displayed a well correlation with those obtained by HPLC analysis.

Similarly in 2013, a nanocomposite made by copper oxide (CuO) and GO (CuOG), dispersed in a mixture of water, ethanol, and Nafion, was drop cast onto SPEs to detect glucose in a flow injection analysis (FIA) system (Sun et al., 2013). Ultralow detection limit of 34.3 nM and an high sensitivity of 2367 $\mu A\ mM^{-1}\ cm^{-2}$ could be attributed to the advantages of FIA as well as the combination of copper catalysis, graphene electronic-networking, and roughness of the SPE surface. In 2014, Dhara et al. (2014) cast SPEs with a dispersion containing platinum nanocube (Pt) and CuO nanoflower decorated rGO. Graphene provided an excellent support for uniform distribution of CuO nanoflower, and contributed by increasing electron transfer flow from CuO to electrode. The oxidation of glucose on the Pt-CuO/rGO-modified SPE occurred at +0.35 V, resulting in a very high sensitivity of 3577 $\mu A\ mM^{-1}\ cm^{-2}$, a limit of detection equal to 0.01 μM, and linear up to 12 mM. The sensor showed better limit of detection and higher sensitivity compared to other carbon-based nanocomposites, e.g. PtNi-graphene, SWCNT/Cu/Nafion, GNS/NiO/DNA. The sensor was employed for the testing of glucose in blood serum, and the results were compared with commercially available glucometer and test strips (OneTouch Ultra, Johnson and Johnson). The same research group developed another enzyme-less glucose sensor, using palladium joined to CuO/rGO instead of Pt (Dhara et al., 2015). The sensor exhibited a very high sensitivity of 3355 $\mu A\ mM^{-1}\ cm^{-2}$, an excellent limit of detection of 30 nM, and a linearity up to 22 mM of glucose, and it greatly compared the OneTouch Ultra glucometer strip.

4.4. Phenol-containing compounds

Detection of phenolic compounds is truly important for industrial, environmental, and food sampling settings. The easy oxidation of phenols with electrodes has prompted the use of electroanalytical methods, i.e. voltammetry and amperometry, for measuring these compounds (Mafatle and Nyokong, 1997). Unfortunately, the anodic detection of phenols has one major drawback: the produced phenoxy radicals rapidly couple to form a passivating polymeric film on the electrode surface, the so-called electrodic fouling (Wang et al., 1998). Consequently, the development of a new surface material, aimed to minimize fouling effects associated with the oxidation of phenol-containing compounds, determined an effective increase in interest in this research field. Regardless, analytical performances such as sensitivity and selectivity always represent important requirements to develop sensing platforms.

Arvinte et al. (2011) studied the electrochemical oxidation of *p*-nitrophenol (*p*-NP), an environmental pollutant, comparing the performances of graphene-Nafion and MWCNT-Nafion dispersions, which acted as SPE-modifiers. The sensitivities of these two nanomaterials toward *p*-NP detection was not dramatically different. MWCNT-SPE displayed an higher background current than graphene leading to a slightly higher limit of detection, 1.3 vs. 0.6 μM for GR-SPE. GR-SPE highlighted lower limit of detection even when compared with nafion-modified glassy carbon electrode (GCE) (Calvo-Marzal et al., 2001), but higher than obtained by using a MWCNT-Nafion/GCE (Huang et al., 2003). In the clinical field, salbutamol, a banned-drug for athletes and a prohibited food additive, has been detected by using a carbon SPE modified with a GR-PEDOT:PSS ink by means of inkjet printing (Karuwan et al., 2012). As obtained from CV studies, GR-PEDOT:PSS-SPE displayed a sensitivity 3-times higher than the PEDOT:PSS-SPE. The oxidation peak current, at +0.78 V, varied linearly in the range from 5 to 550 μM reaching a calculated detection limit of 1.25 μM. The employment of this graphene-based ink allowed to improve the linearity range of salbutamol detection when compared with a work from the same group. In that case, they utilized a CNT-based electrode, embedded in a FIA-based microfluidic device (Karuwan et al., 2009). Furthermore, the GR-PEDOT:PSS-SPE did not show any changes in voltammetric profile after 5 cycles and after 20 successive cycles, just a 4.5% relative standard deviation was obtained, proving the anti-fouling role of graphene. Graphene was used to modify a screen-printed electrode even to improve the detection of buprenorphine, a synthetic narcotic analgesic that acts similarly to methadone, by modifying a SPE with rGO dispersed in DMF (Fakhari et al., 2014). The rGO-SPE response was linear from 0.5 to 100 μM, yielding a detection limit of 0.16 μM. However, in a previous work that described the use of a carbon paste electrode, buprenorphine was detected until 0.02 μM (Garcia-Fernandez et al., 2000). In a recent work from Escarpa's group (Gomez et al., 2015), the use of nanomaterial-based SPEs (commercially and lab-modified electrodes) was investigated and critically evaluated toward the detection of serotonin in presence of melatonin. SPEs modified by drop casting of dispersions containing SWCNT, MWCNT, GNR (reduced graphene nanoribbons), and GON (graphene oxide nanoribbons), were compared with DropSens, manufactured by using MWCNT-, SWCNT-, and graphene-based inks. It was demonstrated that the SPE modified with a GON dispersion resulted in the best sensor to be utilized for such detection. The use of GON-SPE highlighted an obvious electrocatalysis, since the oxidation peak potentials shifted to a lower oxidation values of +0.05 V for serotonine and +0.39 V for melatonine, compared to +0.11 V and +0.45 V at bare SPE. By using GON-SPE, serotonine and melatonine were detected at low limits of detection, respectively 0.4 and 1.1 μM, with a 3-decade linearity, from μ to mM level. These results compared favorably with the limit of detection achieved by using a boron doped diamond (BDD) microelectrode, equal to 1.0 and 2.2 mM respectively for serotonine and melatonine (Patel, 2008). Although the higher electroactive area of graphene, with respect to CNTs serotonin fouled the electrode up to 67% of the initial current. Escarpa highlighted the superior electrocatalysis due to graphene, but Banks' group claimed superior electrochemical signatures of bare SPE over the rGO modified SPE toward the detection of pindolol (Cumba et al., 2015). Bare SPE exhibited a tremendously higher peak height and lower potential than the rGO-SPE. The authors speculated about the reason behind this graphene-low response, and believe it is due to poor electrical wiring of the rGO on the electrode or due to a repulsive interaction with the analyte. The use of bare SPE yielded a limit of detection of 0.097 μM, comparable with a previously reported method based on rGO-GCE (Smarzewska and Ciesielski, 2014). Clearly, the role of graphene cannot be taken for granted. A real comprehension about the effectiveness of graphene-based SPEs for phenolic compound detection, easily oxidable, still needs to be addressed.

4.5. Heavy metals: cadmium and lead

Heavy metals such as cadmium and lead, due to their high toxicity, represent a serious threat to health and the environment. Even exposure to low levels of cadmium and lead can be life-

threatening (Quintana et al., 2012). Anodic stripping voltammetry (ASV) and SPEs represent a consolidated mix to perform the detection of heavy metals, rapidly and sensitively. Graphene, as largely reported also in this review, represents a excellent nanoscale substrate for anchoring metal ions (leading to growth of metal nanoparticles). Similar to CNTs, graphene has a high metal-sorption capacity (Zhao et al., 2011), and its use has grown over the development of such "stripping" printed platforms. ASV is carried out, usually, by forming an alloy between the metal and bismuth, which has almost completely substituted the more toxic mercury (Wang, 2005; Arduini et al., 2010). Bismuth is known to form binary- or multi-component alloys with numerous heavy metals, including lead and cadmium (Krueger et al., 1978). Huangfu et al. (2013) developed a sensor by casting a PSS-dispersed graphene onto a SPE and by using differential pulse stripping voltammetry (DPSV) as the method of detection. Traces of Cd^{2+} and Pb^{2+} were successfully linearly detected up to 120 ppb reaching limit of detection of 0.042 and 0.089 ppb, respectively for the two metals. It highlights the excellent combination between graphene (high electron transfer rate, large surface area and high adsorptive ability) and PSS (cathion-exchange capacity). GR/PSS/Bi-SPE demonstrated a clear enhancement of sensitivity when compared to the GR/PSS-SPE, the PSS/Bi-SPE, and the Bi-SPE. This sensor displayed a wider linear range for both metals when compared with MWCNTs/Nafion/Bi-SPE (Fu et al., 2013), but with respect to the detection limit, the CNT-based SPE allowed to detect cadmium and lead until 0.1 and 0.07 ppb, respectively. Grimaldi et al. (2014) analyzed lead and cadmium ions through the use of commercially-available SPEs made by graphene, SWCNT and MWCNT, comparing them to the graphite SPE. MWCNT-SPE displayed the best peak resolution, and the highest peak intensity, yielding linear ranges between 40 and 100 ppb and limit of detection equal to 29 and 30 ppb for cadmium and lead, respectively. There was an observed increase in the capacitive baseline current for graphene-SPE, with the disappearance of the bismuth peak. This phenomenon could be explained by the high diffusion of Bi^{3+} between graphene

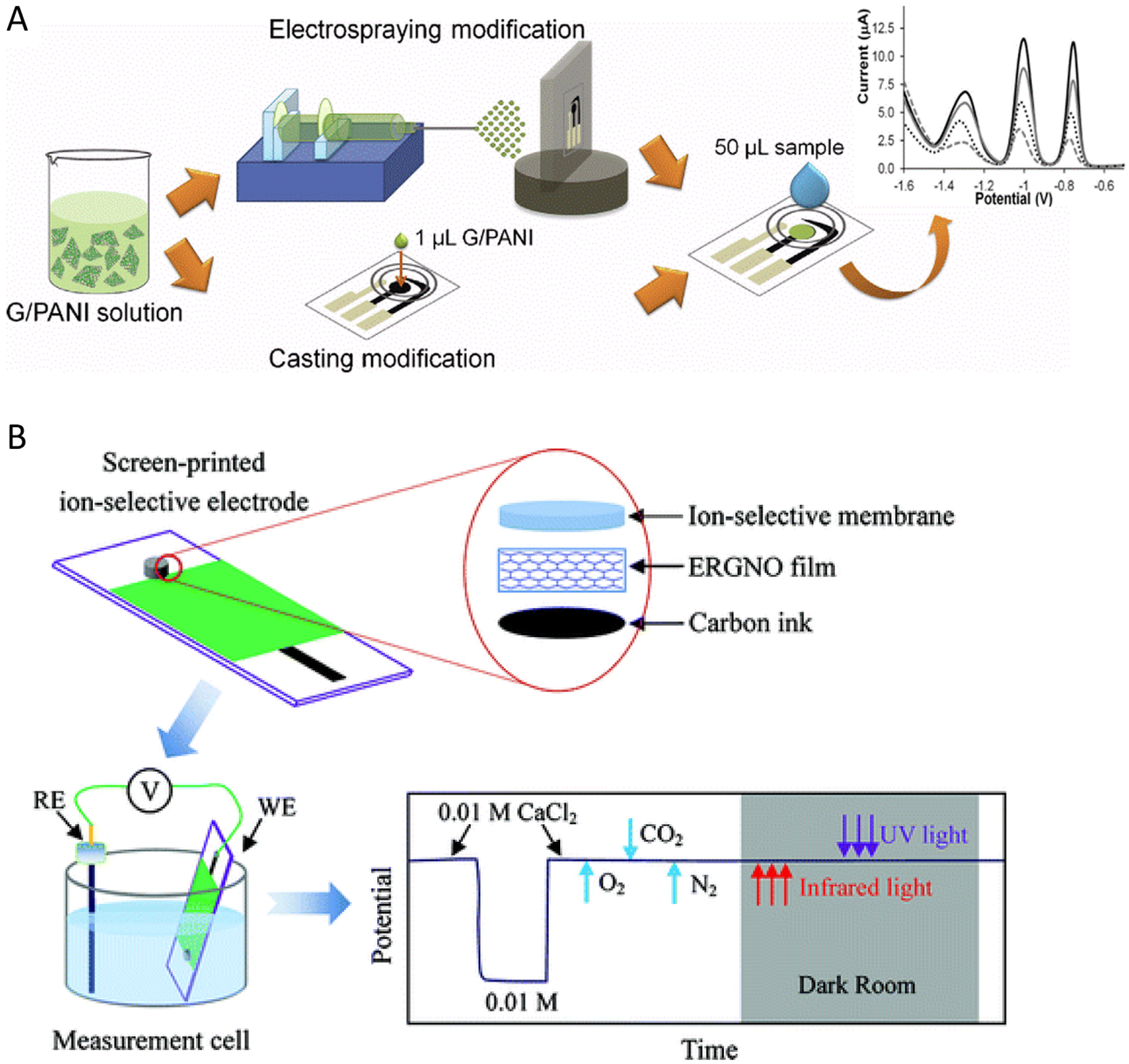

Fig. 6. Schematic representation of: (A) *electrochemical sensor* for simultaneous detection of Zn(II), Cd(II), and Pb(II) using a SPE modified by drop casting with graphene–polyaniline nanocomposite (Ruecha et al., 2015); (B) ion-selective *electrochemical sensor* using graphene as the ion-to-electron transducer fro calcium detection (Ping et al., 2012a). Reprinted with permission from Ref. (Ruecha et al., 2015; Ping et al., 2012a).

layers. A direct comparison was also made between SPEs modified by electrodeposition (ERGNO) and drop casting chemically reduced graphene oxide (CRGNO) (Ping et al., 2014). The stripping response of SPE/ERGNO/Bi was even superior to that of the SPE drop-cast with a chemically reduced GO. The potential reason for this might be the less-uniform film structure obtained from the drop-casting method. The linear range for both metal ions at the disposable bismuth film SPE/ERGNO was from 1 to 60 ppb. The detection limit was 0.5 ppb for cadmium and 0.8 ppb for lead, making this sensor suitable to detect traces of Cd and Pb in milk sample. Subsequently (Wang et al., 2014; Chaiyo et al., 2016), a similar platform based on electrochemically reduced graphene was investigated with the use of ionic liquid doped SPE (IL-SPE). They also evaluated the performance of a GO drop-cast SPE because of its large surface area and capability of metal-adsorption due to the negatively charged functional groups. However, Bi/GR/IL-SPE showed a superior stripping sensitivity with respect to Bi/GO/IL-SPE perhaps due to the poor conductivity of GO. It was found that the peak currents and the concentrations of lead and cadmium exhibited a satisfactory linear correlation in the 1–80 ppb range. Sensitivity and detection limits were 1.1874 μA ppb^{-1} and 0.08 ppb, and 0.7325 μA ppb^{-1} and 0.1 ppb for Cd^{2+} and Pb^{2+}, respectively (Wang et al., 2014). The presence of ionic liquid, well-incorporated to graphene (Chaiyo et al., 2016), allowed to reduce the detectable heavy metal ions with respect to previous paper reported by Wang et al. (2014). Promphet et al. (2015) reported on the use of electrospun graphene/polyaniline/polystyrene (G/PANI/PS) onto SPE. Under optimized experimental conditions, response has been found linear from 10 to 500 ppb with the detection limit of 3.30 ppb and 4.43 ppb for Pb^{2+} and Cd^{2+}, respectively. Although the linearity range appeared as one of the widest when compared with literature, detection limit values compared unfavorably with the previous cited graphene-based sensors but also with respect to some CNT-based SPEs, where detection limit lower than 1 ppb was reported for both stripped metals (Hwang et al., 2008; Afkhami et al., 2013). Recently, Prof. Henry's group described deposited graphene-polyaniline (G/PANI) nanocomposite onto SPEs by means of two procedures, electrospray and drop-casting (Fig. 6A). Electrosprayed G/PANI displayed the best sensitivity, likely due to more uniform particle distribution as compared to drop-casting. G/PANI electrosprayed onto a SPE printed on plastic reflected a linear range up to 300 ppb, with detection limits of 0.1 ppb for both cadmium and lead. Moreover, this platform was also capable to detect simultaneously zinc ion with a limit of detection of 1 ppb (Ruecha et al., 2015).

4.6. Miscellaneous

Screen-printed electrodes based on graphene (in all its forms, and composites) found application towards the detection of various analytical relevant compounds, ranging from environmental pollution to clinical diagnosis. rGO was used in a novel disposable ion selective electrode (ISE) used as the network between ions and the electrode, to selectively detect calcium (Ping et al., 2012a). The disposable electrode showed in Fig. 6B exhibited a Nernstian slope of 29.1 mV/decade, a linearity range of $10^{-5.6}$ to $10^{-1.6}$ M of Ca^{2+} and a detection limit of $10^{-5.8}$ M. The high hydrophobic character of graphene prevented the formation of an aqueous layer inside the electrode (main reason of drift instability). Graphene-ISE displayed a potential drift of 14.7 μV h^{-1} during continuous monitoring (20 h), which was much lower than the 493 μV h^{-1} obtained using a CNT-based solid-contact Ca-ISE (Hernández et al., 2010). Another relevant analyte to detect is caffeine, an antioxidant abundant in coffee. Vasilescu et al. (2015) utilized a DropSens graphite SPE drop-cast with a dispersion of chemically rGO, followed by the deposition of Nafion. Caffeine detection was carried out by means of amperometry (+1.3 V) obtaining a sensitivity of 1.38 μA/μM, a linearity range of 0.29–2.58, and a detection limit of 0.22 μM. Despite the modification with the double layer, high potential is still required to oxidize caffeine. Graphene oxide nanosheets (GONs) has been recently utilized in combination with titanium dioxide nanofibers (TNFs) as a SPE modifier to detect adenine, one of the building blocks of nucleic acids. Authors argued for a synergistic effect between TNFs and GONs, because of the decrease of overpotential and the increase of the peak current, even if no results have been reported on the use of TNFs/SPE. By DPV analysis, adenine in presence of the interfering guanine was linearly detected in two ranges, 0.1–1 and 1–10 μM, with detection limit of 1.71 nM (Arvand et al., 2016). Other graphene based composites as SPE modifiers have been also recently reported in literature including graphene oxide/ZnO nanorods for levodopa and tyrosine detection (Beitollahi and Garkani Nejad, 2016), graphene oxide/carbon nanotubes/gold nanoparticles for bisphenol A (Wang et al., 2015), polyaniline/graphene quantum dot for Cr (VI) (Punrat et al., 2016), graphene oxide/pyrrole and pyrrole-3-carboxylic acid as nano-molecularly imprinted polymer for cardiac troponin T detection (Silva et al., 2016).

5. Remarks and conclusions

Screen-printed electrodes (SPEs), without any doubt, show a plethora of advantages with respect to the most used glassy carbon electrodes such as the easy customisation with graphene, cost-effectiveness, miniaturization, the requirement of only some μL of sample, suitability for *in field* analysis, and the absence of surface pre-treatment or polishing. Their features make this type of electrode extremely competitive with respect to other classical electrodes, which is why many papers have been devoted to graphene based screen-printed (bio)sensor development for detection of several compounds (Table 1). The use of graphene in analytical field encompasses graphene as a material for SPE fabrication and as label or loading agent as well. The capability of high loading properties was firstly investigated in drug delivery, and taking inspiration by the outstanding results achieved, the loading properties of graphene were employed for electrochemical sensing tool development. Du et al. (2011) have highlighted their effort of using graphene for sensitivity enhancement and wider linear range, owing it to the capability to load higher units of enzyme with respect to GO-less format, in the same route Li et al. (2015) have chosen GO to control the decoration of nanoparticles without aggregation for immuno-chain labeling.

These features have been also exploited to improve the electrochemical performance of inorganic composites. Many platforms have been reported by taking advantage of the high surface-to-area ratio of graphene. Particularly, graphene has shown to help the homogeneous deposition of metal-nanoparticles on the SPE surface, avoiding the evolution of NPs cluster/aggregate. Glucose enzymeless detection is a main example. Pd-, Pt-, Cu-nanoparticles have been efficiently dispersed in a graphene network, highlighting improved sensitivity (Sun et al., 2013; Dhara et al., 2014, 2015).

These results have underscored the role of graphene not only for signal enhancement thanks to multienzyme labeling, but also as a label, using inherently electroactive property of GO nanoplatelets to supply the analytical signal (Bonanni et al., 2012). Furthermore, as highlighted by Pumera's group GO nanoplatelets is not only a new label for biosensors, but also possess many advantages over metal nanoparticle labels by avoiding use of toxic chemicals; such as the case of quantum dot labels, where concentrated acid solution HCl/HNO_3 is required for measurement (Loo et al., 2013).

Table 1
Several analytes detected by means of graphene-based screen-printed electrochemical (bio)sensors.

Analyte	(Bio)sensor	Graphene	LOD	Linear range	Real sample	Ref.
AA, DA, UA	rGO incorporated into a carbon ink and screen-printed. Detection by DPV at −0.05 V, 0.15 V, 0.3 V.	rGO. GO reduced via hydrazine.	0.95 μM, 0.12 μM, 0.20 μM	4.0–4500 μM, 0.5–2000 μM, 0.8–2500 μM	–	Ping et al., 2012b
AA, LD, UA	GNRred drop cast onto SPE. Detection by DPV at 0.08 V, 0.27 V, 0.39 V.	GNRred. Unzipped MWCNTs under oxidizing conditions. Reduced by hydrazine.	5 μM (UA)	1–5 mM, 10–50 μM, 10–50 μM	Urine	Martin et al., 2015
Adenine	TNFs/GONs drop cast onto SPE. Detection by DPV at 0.858 V.	GONs. Electrochemical graphite rod exfoliation.	1.71 nM	0.1–1 and 1–10 μM	Plasmid	Arvand et al., 2016
α-fetoprotein	Capture antibody immobilized onto GO-SPE. Binding with α-fetoprotein was evaluated by adding CuS/GO labeled with signal antibody. Detection by chrono-amperometry at −0.27 V.	GO.	0.5 pg mL^{-1}	0.001–10 ng mL^{-1}	Blood serum	Li et al., 2015
β-lactoglobulin	Immunological chain immobilised onto GR-SPE derivatized. Detection by DPV at around 0 V.	Disposable GR-SPE commercial available.	0.85 ng L^{-1}	1 pg mL^{-1} –100 ng mL^{-1}	Cake, cheese snacks, sweet biscuit	Eissa et al., 2012
Buprenorphine	rGO drop cast onto SPE. Detection by DPV at 0.38 V.	rGO. GO reduced by sodium borohydride.	0.16 μM	0.50–100 μM	Urine	Fakhari et al., 2014
Cadmium, Lead	GR/PSS drop cast onto SPE. Bi-film electrodeposited onto GR/PSS-SPE. Detection by DPV performed in the potential range from −1.15 to −0.35 V.	Graphene powder.	0.042 ppb, 0.089 ppb	0.5–120 ppb (both)	Lake and tap water	Huangfu et al., 2013
	Electroreduction of GO onto SPE. Bi-film electrodeposited onto ERGO-SPE. Detection by SWASV from −1.0 to −0.3 V.	ERGO.	0.5 ppb, 0.8 ppb	1–60 ppb (both)	Milk	Ping et al., 2014
	Electrochemical reduction of GO onto the IL-SPE. Detection by SWASV from −1.1 to −0.3 V.	rGO. GO reduced via electrochemically mode.	0.08 ppb, 0.1 ppb	1–80 ppb (both)	Rice	Wang et al., 2014
	Electrospun GR/PANI/PS nanoporous fiber onto SPE. Detection by Bi-film electrodeposited onto GR/PANI/PS-SPE by SWASV from −1.0 to −0.2 V.	Graphene powder.	4.43 ppb, 3.30 ppb	10–500 ppb (both)	River water	Promphet et al., 2015
Caffeine	rGO and Nafion were drop cast onto SPE. Detection by amperometric mode at 1.3 V.	rGO. GO reduced via hydrazine.	0.22 μM	0.29–2.58 μM	Coffee	Vasilescu et al., 2015
Cancer biomarkers: AFP, CEA, CA125, CA153	Immunological chain immobilised onto paper based printed sensor modified with GO. Detection by DPV at −0.5 V.	GO.	1 pg mL^{-1} (AFP, CA125) 5 pg mL^{-1} (CEA, CA153)	0.001–100 ng mL^{-1} (AFP, CA125) 0.005–100 ng mL^{-1} (CEA, CA153)	–	Wu et al., 2013
Clenbuterol	Ab immobilised at Fe_3O_4-Au magnetic Nanoparticles coupled with GR-SPE. Detection by DPV at 0.1 V.	rGO. GO reduced via hydrazine.	0.22 ng mL^{-1}	0.5–200.0 ng mL^{-1}	Pork samples	Yang et al., 2014
Fructose	Fructose dehydrogenase immobilised with osmium-polymer on Gr-SPE. Detection in amperometric mode at 0.15 V.	Disposable Gr-SPE commercial available.	0.8 μM	0.1–8 mM	Honey, red wine, orange juice, pine-apple juice, tomato juice, apple juice, cola, energy drink	Antiochia and Gorton, 2014
Glucose	GOX immobilized on ERGO/IL-SPE. The enzymatic product (H_2O_2) was amperometrically detected at −0.2 V.	ER-GNO. GO reduced via electrochemically mode.	1.0 μM	5.0 μM–10.0 mM	Milk	Ping et al., 2011
	GOX mixed with Gr/PANI/AuNPs composite and drop-cast onto SPE. Detection in DPV mode at −0.42 V.	rGO.	0.1 mM	0.2–11.2 mM	Whole blood	Kong et al., 2014
	GOX immobilized on GR-SPE. Direct electron transfer at Gr-SPE. Detection in amperometric mode at −0.4 V.	Graphene-PEDOT:PSS	0.3 μM	20–900 μM	–	Wisitsoraat et al., 2013
	GOX immobilized on Gr-SPE, Direct electron transfer at GR-SPE. Detection by amperometry at −0.4 V.	Sonochemical-assisted solvent exfoliation of graphite flakes.	28.3 μM	0.1–1 mM,	–	Chia et al., 2015

Table 1 (*continued*)

Analyte	(Bio)sensor	Graphene	LOD	Linear range	Real sample	Ref.
	Nanocomposite of CS-rGO-NiNPs electrodeposited onto SPE. Detection by amperometric mode at 0.6 V.	rGO.	4.1 μM	0.2–9 mM	Urine	Yang et al., 2013
	Nanocomposite of Pt-CuO/rGO drop cast onto SPE. Detection by amperometric mode at 0.6 V.	rGO.	0.01 μM	up to 12 mM	Blood serum	Dhara et al., 2014
hCG	Immunological chain immobilised onto GR-SPE-PANI. Detection by EIS	Disposable GR-SPE commercial available.	0.286 pg mL^{-1}	0.001–50 ng mL^{-1}	Urine	Teixeira et al., 2014
HIV-1	Electrochemical molecular beacon, combined with a nafion–graphene composite film modified SPE	Graphene powder.	5 nM	40 nM–2.56 μM	Blood serum	Li et al., 2014
Hydrogen peroxide	HRP immobilized at Fe_3O_4-Au magnetic nanoparticles coupled with GR-SPE. Detection by amperometric mode at −0.3 V.	rGO. GO reduced by hydrazine.	12 μM	20 μM–2.5 mM	Contact lens care solution	Xin et al., 2013
	LS deposition of ODA-rGO-ODA-PB-DODA onto SPE. Detection by amperometric mode at 0 V.	rGO. GO reduced by sodium borohydride.	2 μM	5–1000 μM	Mouth wash solution	Michopoulos et al., 2014
	N-GRNRs drop cast onto SPE. Detection by amperometric mode at −0.4 V.	N-GRNRs. Unzipped MWCNTs under oxidizing conditions. Doping with nitrogen by a low-temperature hydrothermal method.	1.72 μM.	5–2785 μM	–	Shi et al., 2015
	Graphene-PEDOT:PSS inkjet-printed onto SPE. Detection by CV, signal at 0.9 V.	Graphene-PEDOT:PSS	194.37 μM	1.3–7.6 mM	–	Sriprachuabwong et al., 2012
miRNAs	SPE modified with rGO to immobilize oligonucleotide. An antibody directed to DNA. RNA hybrids was employed with HRP. Detection by SWV at around 0.1 V.	GO was reduced by epigallocatechin-3-gallate	10 fM	Up to 1 nM	–	Tran et al., 2014
Okadaic acid	Immunological chain immobilised onto GR-SPE derivatized. Detection by DPV (peak at around 0.0 V)	Disposable GR-SPE commercial available.	19 ng L^{-1}	Up to 5 μg L^{-1}	Mussels	Eissa and Zourob, 2012
p53 (S392) protein (tumor suppressor)	Immunological chain immobilised onto printed sensor using GO as loading agent for Ab_2 and HRP. Detection by SWV at −0.3 V.	GO.	0.01 nM	0.02–2 nM	Human plasma	Du et al., 2011
p-nitrophenol	GR and Nafion were drop cast onto SPE. Detection by DPV at 0.96 V.	Graphene powder.	0.6 μM	10 μM–0.62 mM	–	Arvinte et al., 2011
Prostate specific antigen	Immunological chain was immobilized onto paper based SPE modified with GR. Detection by LSSV at 0.1 V.	GS.	0.46 pg mL^{-1}	0.002 ng mL^{-1}–2.0 μg mL^{-1}.	Blood serum	Yan et al., 2012
TNF-α	Determination of TNF-α antigen was based on obstruction to the electrocatalytic oxidation of catechol by Ag@PtGRs after binding to the surface of the electrode through interaction with the aptamer. Detection by DPV at 0.2 V.	rGO. GO reduced by sodium borohydride.	2.07 pg mL^{-1}	Up to 60 pg mL^{-1}	Blood serum	Mazloum-Ardakani et al., 2015

All potentials are vs. Ag/AgCl.

GR=Graphene; GO=Graphene oxide; rGO=Reduced graphene oxide; GS=Graphene sheets; GOX=Glucose oxidase, PEDOT:PSS=Poly(3,4 ethylenedioxythiophene):poly-styrene-sulfonic acid; HRP=horseradish peroxidase; FDH=Fructose dehydrogenase; AFP=Alpha-fetoprotein, CEA=Carcinoembryonic antigen, CA125=Cancer antigen 12%, CA153=Carbohydrate antigen 153; Au-SPE=Gold-SPE; hCG=Human chorionic gonadotropin; SWV=Square wave voltammetry; EIS=Electrochemical impedance spectroscopy; Ab=Antibody; CuS/GO=CuS nanoparticle-decorated graphene; LSSV=Linear sweep stripping voltammetry; ODA=Octadecylamine; DODA=Dimethyldioctadecylammonium; CS=Chitosan; NiNPs=Nickel nanoparticles; Pt=Platinum nanocubes; PB=Prussian Blue; Pd=Palladium nanoparticles; LS=Langmuir-Schaefer; N-GrNRs=Nitrogen-doped graphene nanoribbons; AA=Ascorbic acid; UA=Uric acid; DA=Dopamine; LD=Levodopa; GNRred=Graphene nanoribbons reduced; GR/PSS=Graphene-poly(sodium 4 styrenesulfonate); ERGO=Electrochemically reduced graphene oxide; IL=Ionic liquids; GR/PANI/PS=graphene/polyaniline/polystyrene; TNFs/GONs=Titanium dioxide nanofibers/graphene oxide nanosheets.

The capabilities of graphene reported above, as a loading agent and a sustainable label, should be considered together with graphene criticisms.

The criticism is related to the source of graphene, having graphene and its related materials different properties depending on preparation methods. A clear picture is reported by Pumera and coworkers (Ambrosi et al., 2014), who highlight that the gathering of different graphene materials can be enclosed under a single umbrella of "graphene". They have emphasized how the trend of classifying all graphene-related materials as "graphene" can contribute to the confusion among scientists not specialized in graphene research, and they have suggested to report in each work the characterization of graphene based material utilized in order to correlate the results obtained with the exact nature of material employed.

In this regard, we have recently performed a comparative study using SPEs modified by drop casting with carbon black, SWCNTs–COOH, GO, and rGO. The carbon nanomaterials employed were characterized by X-ray photoelectron and Raman spectroscopy, while the modified SPEs were characterized morphologically. The electrochemical behavior of nanomodified sensors was tested using cyclic voltammetry, amperometry, and electrochemical impedance spectroscopy. The results obtained for amperometric detection of NADH, ascorbic acid, and cysteine have demonstrated that graphene modified SPEs were less performant than SPEs modified with SWCNTs–COOH and carbon black, and between GO and rGO, SPEs modified with rGO has shown superior sensitivity (Cinti et al., 2015). Regarding the non-outstanding electrochemical performance of the graphene modified SPE observed, some comments need to be made. Apart from the enhancement of electrochemical performances demonstrated in the several papers with GR-SPE, other works highlighted no competitive electrochemical behavior of the modified sensor. For instance, Banks and coworkers have reported the absence of electroanalytical performance improvements in the pindolol detection using SPE modified by drop casting with a dispersion of reduced graphene oxide compared to bare SPE (Cumba et al., 2015). In the same context, Pumera reported that the initial excitement concerning the performance of the carbon nanotubes and graphene materials was replaced with increasing crises caused by the use of impure materials (Pumera, 2012).

The different behaviors obtained with GR-SPEs can be ascribed to the different graphene samples employed. To this end, several factors affect the electrochemical properties such as: i) metallic impurities that can be eventually present in graphene and, if present in different contents, originated from the staring material, where these impurities have the capability to alter the electrochemical behavior, as observed some years ago in the case of carbon nanotubes by Compton's group (Ambrosi et al., 2012a, 2012b; Banks et al., 2006), ii) the structure, since multi layer structure can have different electrochemistry with respect to the single layer structure (Goh and Pumera, 2010), iii) amount of oxygen because the presence of a higher amount of oxygen could reduce the electron transfer as observed in graphite (Ambrosi et al., 2014; Ji et al., 2006), iv) the number of defect sites, taking into account that edge plane sites are more electroactive than basal plane sites, and pristine graphene is characterized by low density of defects (Ambrosi et al., 2014), and v) the amount of graphene loaded onto the working electrode surface because higher amount of graphene can block the electroactive edge sites reducing the electron transfer rate (Brownson et al., 2011).

We can conclude that graphene can be considered an outstanding polyedric material, since it can be used to tailor the electrochemical properties of a screen-printed electrode, as well as act as a label and loading agent for biomolecules and inorganic nanomaterials, exploiting its high surface area and easy functionalization.

If K.S. Novoselov described graphene as *more than just a flat crystal*, using graphene in the sensing area could be seen as a *kaleidoscope*. Depending on its configuration, graphene confers different features for sensing tools.

Acknowledgments

This work was supported by Italian Minister of Defence, Aptamer BW. The authors thank Julian Ramirez for revising the English manuscript.

References

Afkhami, A., Ghaedi, H., Madrakian, T., Rezaeivala, M., 2013. Electrochim. Acta 89, 377–386.
Albareda-Sirvent, M., Merkoci, A., Alegret, S., 2000. Sens. Actuators, B 69, 153–163.
Ambrosi, A., Chua, C.K., Khezri, B., Sofer, Z., Webster, R.D., Pumera, M., 2012a. Proc. Natl. Acad. Sci. 109, 12899–12904.
Ambrosi, A., Chee, S.Y., Khezri, B., Webster, R.D., Sofer, Z., Pumera, M., 2012. Angew. Chem., Int. Ed. (51), 500–503.
Ambrosi, A., Chua, C.K., Bonanni, A., Pumera, M., 2014. Chem. Rev. 114, 7150–7188.
Antiochia, R., Gorton, L., 2014. Sens. Actuators, B 195, 287–293.
Apetrei, I.M., Apetrei, C., 2016. Int. J. Nanomed. 11, 1859–1866.
Arduini, F., Calvo, J.Q., Amine, A., Palleschi, G., Moscone, D.A., 2010. Trac. Trends Anal. Chem. 29, 1295–1304.
Arduini, F., Forchielli, M., Amine, A., Neagu, D., Cacciotti, I., Nanni, F., Moscone, D., Palleschi, G., 2015. Microchim. Acta 182, 643–651.
Arduini, F., Micheli, L., Moscone, D., Palleschi, G., Piermarini, S., Ricci, F., Volpe, G., 2016. Trac. Trends Anal. Chem. 79, 114–126.
Arvand, M., Ghodsi, N., Zanjanchi, M.A., 2016. Biosens. Bioelectron. 77, 837–844.
Arvinte, A., Mahosenaho, M., Pinteala, M., Sesay, A.M., Virtanen, V., 2011. Microchim. Acta 174, 337–343.
Avouris, P., Dimitrakopoulos, C., 2012. Mater. Today 15, 86–97.
Balandin, A. A. ,2011. Thermal properties of graphene and nanostructured carbon materials. Nat. Mater. 10(8), 569–581.
Banks, C.E., Crossley, A., Salter, C., Wilkins, S.J., Compton, R.G., 2006. Angew. Chem., Int. Ed. 45, 2533–2537.
Beitollahi, H., Garkani Nejad, F., 2016. Electroanalysis . http://dx.doi.org/10.1002/elan.201600143.
Bonaccorso, F., Sun, Z., Hasan, T., Ferrari, A.C., 2010. Nat. Photonics 4, 611–622.
Bonanni, A., Chua, C.K., Zhao, G., Sofer, Z., Pumera, M., 2012. ACS Nano 6, 8546–8551.
Brownson, D.A.C., Munro, L.J., Kampouris, D.K., Banks, C.E., 2011. RSC Adv. 1, 978–988.
Brownson, D.A.C., Kampouris, D.K., Banks, C.E., 2012. Chem. Soc. Rev. 41, 6944–6976.
Calvert, P., 2001. Chem. Mater. 13, 3299–3305.
Calvo-Marzal, P., Rosatto, S.S., Granjeiro, P.A., Aoyama, H., Kubota, L.T., 2001. Anal. Chim. Acta 441, 207–217.
Carocho, M., Ferreira, I.C., 2013. Food Chem. Toxicol. 51, 15–25.
Chaiyo, S., Mehmeti, E., Žagar, K., Siangproh, W., Chailapakul, O., Kalcher, K., 2016. Anal. Chim. Acta 918, 26–34.
Chen, W., Cai, S., Ren, Q.Q., Wen, W., Zhao, Y.D., 2012. Analyst 137, 49–58.
Chen, S., Yuan, R., Chai, Y., Hu, F., 2013. Microchim. Acta 180, 15–32.
Chia, J.S.Y., Tan, M.T., Khiew, P.S., Chin, J.K., Siong, C.W., 2015. Sens. Actuators, B 210, 558–565.
Cinti, S., Arduini, F., Carbone, M., Sansone, L., Cacciotti, I., Moscone, D., Palleschi, G., 2015. Electroanalysis 27, 2230–2238.
Cumba, L.R., Smith, J.P., Brownson, D.A., Iniesta, J., Metters, J.P., do Carmo, D.R., Banks, C.E., 2015. Analyst 140, 1543–1550.
Das, R., Harrop, P., 2013. Printed, organic & flexible electronics: forecasts, players & opportunities 2013–2023, IDTechEx Report.
Deegan, R.D., Bakajin, O., Dupont, T.F., Huber, G., Nagel, S.R., Witten, T.A., 1997. Nature 389, 827–829.
Dhara, K., Thiagarajan, R., Nair, B.G., Thekkedath, G.S.B., 2015. Microchim. Acta 182, 2183–2192.
Dominguez Renedo, O., Alonso-Lomillo, M.A., Arcos Martinez, M.J., 2007. Talanta 73, 202–219.
Dreyer, D.R., Park, S., Bielawski, C.W., Ruoff, R.S., 2010. Chem. Soc. Rev. 39, 228–240.
Du, D., Wang, L., Shao, Y., Wang, J., Engelhard, M.H., Lin, Y., 2011. Anal. Chem. 83, 746–752.
Eda, G., Fanchini, G., Chhowalla, M., 2008. Nat. Nanotechnol. 3, 270–274.
Eissa, S., Zourob, M., 2012. Nanoscale 4, 7593–7599.
Eissa, S., Tlili, C., L'Hocine, L., Zourob, M., 2012. Biosens. Bioelectron. 38, 308–313.
Escarpa, A., 2012. Chem. Rec. 12, 72–91.
Fakhari, A.R., Sahragard, A., Ahmar, H., 2014. Electroanalysis 26, 2474–2483.
Fu, L., Li, X., Yu, J., Ye, J., 2013. Electroanalysis 25, 567–572.
Garcia-Fernandez, M.A., Fernandez-Abedul, M.T., Costa-Garcia, A., 2000.

Electroanalysis 12, 483–489.
Geim, A.K., Novoselov, K.S., 2007. Nat. Mater. 6, 183–191.
Gilje, S., Han, S., Wang, M., Wang, K.L., Kaner, R.B., 2007. Nano Lett. 7, 3394–3398.
Goh, M.S., Pumera, M., 2010. Anal. Chem. 82, 8367–8370.
Gomez, F.J.V., Martín, A., Silva, M.F., Escarpa, A., 2015. Microchim. Acta 182, 1925–1931.
Greiner, A., Wendorff, J.H., 2007. Angew. Chem. Int. 46, 5670–5703.
Grimaldi, A., Heijo, G., Méndez, E., 2014. Electroanalysis 26, 1684–1693.
Guiberteau-Cabanillas, A., Godoy-Cancho, B., Bernalte, E., Tena-Villares, M., Guiberteau Cabanillas, C., Martínez-Cañas, M.A., 2015. Electroanalysis 27, 177–184.
Hernández, R., Riu, J., Rius, F.X., 2010. Analyst 135, 1979–1985.
Huang, W., Yang, C., Zhang, S., 2003. Anal. Bioanal. Chem. 375, 703–707.
Huangfu, C., Fu, L., Li, Y., Li, X., Du, H., Ye, J., 2013. Electroanalysis 25, 2238–2243.
Hwang, G.H., Han, W.K., Park, J.S., Kang, S.G., 2008. Talanta 76, 301–308.
Istrate, O.M., Rotariu, L., Bala, C., 2016. Microchim. Acta 183, 57–65.
Jahani, S., Beitollahi, H., 2016. Electroanalysis . http://dx.doi.org/10.1002/elan.201501136.
Ji, X.B., Banks, C.E., Crossley, A., Compton, R.G., 2006. Chem. Phys. Chem. 7, 1337–1344.
Jian, J.-M., Liu, Y.-Y., Zhang, Y.-L., Guo, X.-S., Cai, Q., 2013. Sensors 13, 13063–13075.
Karuwan, C., Wisitsoraat, A., Maturos, T., Phokharatkul, D., Sappat, A., Jaruwongrungsee, K., Lomas, T., Tuantranont, A., 2009. Talanta 79, 995–1000.
Karuwan, C., Sriprachuabwong, C., Wisitsoraat, A., Phokharatkul, D., Sritongkham, P., Tuantranont, A., 2012. Sens. Actuators B 161, 549–555.
Karyakin, A.A., Karyakina, E.E., Gorton, L., 2000. Anal. Chem. 72, 1720–1723.
Kong, F.-Y., Gu, S.-X., Li, W.-W., Chen, T.-T., Xu, Q., Wang, W., 2014. Biosens. Bioelectron. 56, 77–82.
Kosynkin, D.V., Higginbotham, A.L., Sinitskii, A., Lomeda, J.R., Dimiev, A., Price, B.K., Tour, J.M., 2009. Nature 458, 872–876.
Krueger, J., Winkler, P., Luderitz, E., Luek, M., 1978. Bismuth alloys and bismuth compounds. In: Grayson, M. (Ed.), Ullman's Encyclopedia of Industrial Technology 3. Wiley, New York.
Laschi, S., Mascini, M., 2006. Med. Eng. Phys. 28, 934–943.
Lawal, A.T., 2015. Talanta 131, 424–443.
Lee, C., Wei, X.D., Kysar, J.W., Hone, J., 2008. Science 321, 385–388.
Lee, S.X., Lim, H.N., Ibrahim, I., Jamil, A., Pandikumar, A., Huang, N.M., 2016. Biosens. Bioelectron. . http://dx.doi.org/10.1016/j.bios.2015.12.030
Li, D., Mueller, M.B., Gilje, S., Kaner, R.B., Wallace, G.G., 2008a. Nat. Nanotechnol. 3, 101–105.
Li, X., Zhang, G., Bai, X., Sun, X., Wang, X., Wang, E., Dai, H., 2008b. Nat. Nanotechnol. 3, 538–542.
Li, M., Li, Y.T., Li, D.W., Long, Y.T., 2012. Anal. Chim. Acta 734, 31–44.
Li, B., Li, Z., Situ, B., Dai, Z., Liu, Q., Wang, Q., Gu, D., Zheng, L., 2014. Biosens. Bioelectron. 52, 330–336.
Li, L., Zhang, L., Yu, J., Ge, S., Song, X., 2015. Biosens. Bioelectron. 71, 108–114.
Lin, Y.M., Dimitrakopoulos, C., Jenkins, K.A., Farmer, D.B., Chiu, H.Y., Grill, A. and Avouris, P., 2010. 100-GHz transistors from wafer-scale epitaxial graphene. Science, 327(5966), .662-662.
Loo, A.H., Bonanni, A., Pumera, M., 2013. Nanoscale 5, 7844–7848.
Lu, L., Liu, B., Leng, J., Wang, K., Ma, X., Wu, S., 2016. Microchim. Acta 183, 837–843.
Mafatle, T., Nyokong, T., 1997. Anal. Chim. Acta 354, 307–314.
Martin, A., Escarpa, A., 2014. Trends Anal. Chem. 56, 13–26.
Martin, A., Hernández-Ferrer, J., Martínez, M.T., Escarpa, A., 2015. Electrochim. Acta 172, 2–6.
Mayorov, A.S., Gorbachev, R.V., Morozov, S.V., Britnell, L., Jalil, R., Ponomarenko, L. A., Blake, P., Novoselov, K.S., Watanabe, K., Taniguchi, T., Geim, A.K., 2011. Nano Lett. 11, 2396–2399.
Mazloum-Ardakani, M., Hosseinzadeh, L., Taleat, Z., 2015. Biosens. Bioelectron. 74, 30–36.
McAllister, M.J., Li, J.-L., Adamson, D.H., Schniepp, H.C., Abdala, A.A., Liu, J., Herrera-Alonso, M., Milius, D.L., Car, R., Prud'homme, R.K., Aksay, I.A., 2007. Chem. Mater. 19, 4396–4404.
Metters, J.P., Kadara, R.O., Banks, C.E., 2011. Analyst 136, 1067–1076.
Michopoulos, A., Kouloumpis, A., Gournis, D., Prodromidis, M.I., 2014. Electrochim. Acta 146, 477–484.
Novoselov, K.S., Geim, A.K., Morozov, S.V., Jiang, D., Zhang, Y., Dubonos, S.A., Grigorieva, I.V., Firsov, A.A., 2004. Science 306, 666–669.
Novoselov, K.S., Fal'ko, V.I., Colombo, L., Gellert, P.R., Schwab, M.G., Kim, K., 2012. Nature 490, 192–200.
Obraztov, A.N., 2009. Nat. Nanotechnol. 4, 212–213.
Paredes, J.I., Villar-Rodil, S., Martinez-Alonso, A., Tascon, J.M.D., 2008. Langmuir 24, 10560–10564.
Patel, B.A., 2008. Analyst 133, 516–524.
Ping, J., Wang, Y., Fan, K., Wu, J., Ying, Y., 2011. Biosens. Bioelectron. 28, 204–209.
Ping, J., Wang, Y., Ying, Y., Wu, J., 2012a. Anal. Chem. 84, 3473–3479.
Ping, J., Wu, J., Wang, Y., Ying, Y., 2012b. Biosens. Bioelectron. 34, 70–76.
Ping, J., Wang, Y., Wu, J., Ying, Y., 2014. Food Chem. 151, 65–71.
Privett, B.J., Shin, J.H., Schoenfisch, M.H., 2008. Anal. Chem. 80, 4499–4517.
Prodromidis, M.I., 2010. Electrochim. Acta 55, 4227–4233.
Promphet, N., Rattanarat, P., Rangkupan, R., Chailapakul, O., Rodthongkum, N., 2015. Sens. Actuators, B 207, 526–534.
Pumera, M., 2012. Chem. Rec. 12, 201–213.
Punrat, E., Maksuk, C., Chuanuwatanakul, S., Wonsawat, W., Chailapakul, O., 2016. Talanta 150, 198–205.
Quintana, J.C., Arduini, F., Amine, A., van Velzen, K., Palleschi, G., Moscone, D., 2012. Anal. Chim. Acta 736, 92–99.
Randviir, E.P., Brownson, D.A.C., Metters, J.P., Kadara, R.O., Banks, C.E., 2014. Phys. Chem. Chem. Phys. 16, 4598–4611.
Ricci, F., Palleschi, G., 2005. Biosens. Bioelectron. 21, 389–407.
Ruecha, N., Rodthongkum, N., Cate, D.M., Volckens, J., Chailapakul, O., Henry, C.S., 2015. Anal. Chim. Acta 874, 40–48.
Scognamiglio, V., 2013. Biosens. Bioelectron. 47, 12–25.
Shao, Y., Wang, J., Wu, H., Liu, J., Aksay, I.A., Lin, Y., 2010. Electroanalysis 22, 1027–1036.
Shi, L., Niu, X., Liu, T., Zhao, H., Lan, M., 2015. Microchim. Acta 182, 2485–2493.
Silva, B.V., Rodríguez, B.A., Sales, G.F., Maria Del Pilar, T.S., Dutra, R.F., 2016. Biosens. Bioelectron. 77, 978–998.
Singh, M., Haverinen, H.M., Dhagat, P., Jabbour, G.E., 2010. Adv. Mater. 22, 673–685.
Smarzewska, S., Ciesielski, W., 2014. Anal. Methods 6, 5038–5046.
Smirnoff, N., 2000. Curr. Opin. Plant Biol. 3, 229–235.
Sriprachuabwong, C., Karuwan, C., Wisitsorrat, A., Phokharatkul, D., Lomas, T., Sritongkham, P., Tuantranont, A., 2012. J. Mater. Chem. 22, 5478–5485.
Stankovich, S., Dikin, D.A., Dommett, G.H.B., Kohlhaas, K.M., Zimney, E.J., Stach, E.A., Piner, R.D., Nguyen, S.T., Ruoff, R.S., 2006. Nature 442, 282–286.
Stankovich, S., Dikin, D.A., Piner, R.D., Kohlhaas, K.A., Kleinhammes, A., Jia, Y., Wu, Y., Nguyen, S.T., Ruoff, R.S., 2007. Carbon 45, 1558–1565.
Stenman, U.H., Alfthan, H., Hotakainen, K., 2004. Clin. Biochem. 37, 549–561.
Sun, X., Liu, Z., Welsher, K., Tucker Robinson, J., Goodwin, A., Zaric, S., Dai, H., 2008. Nano. Res. 1, 203–212.
Sun, C.L., Cheng, W.L., Hsu, T.K., Chang, C.W., Chang, J.L., Zen, J.M., 2013. Electrochem. Commun. 30, 91–94.
Taleat, Z., Khoshroo, A., Mazloum-Ardakani, M., 2014. Microchim. Acta 181, 865–891.
Teixeira, S., Conlan, R.S., Guy, O.J., Goreti, M., Sales, F., 2014. J. Mater. Chem. B 2, 1852–1865.
Thevenot, D.R., Toth, K., Durst, R.A., Wilson, G.S., 2001. Biosens. Bioelectron. 16, 121–131.
Thiyagarajan, N., Chang, J.L., Senthilkumar, K., Zen, J.M., 2014. Electrochem. Commun. 38, 86–90.
Torres, J.A., Kaner, R.B., 2014. Nat. Mater. 13, 328–329.
Tran, H.V., Piro, B., Reisberg, S., Huy Nguyen, L., Dung Nguyen, T., Duc, H.T., Pham, M. C., 2014. Biosens. Bioelectron. 62, 25–30.
Tsiafoulis, C.G., Trikalitis, P.N., Prodromidis, M.I., 2005. Electrochem. Commun. 7, 1398–1404.
Turner, A.P.F., 2013. Chem. Soc. Rev. 42, 3184–3196.
Updike, S.J., Hicks, G.P., 1967. Nature 214, 986–988.
Vasilescu, I., Eremia, S.A., Penu, R., Albu, C., Radoi, A., Litescu, S.C., Radu, G.L., 2015. RSC Adv. 5, 261–268.
Virojanadara, C., Syväjarvi, M., Yakimova, R., Johansson, L.I., Zakharov, A.A., Balasubramanian, T., 2008. Phys. Rev. B 78, 245403–245408.
Visone, R., Croce, C.M., 2009. Am. J. Pathol. 174, 1131–1138.
Wang, J., 2005. Electroanalysis 17, 1341–1346.
Wang, J., 2008. Chem. Rev. 108, 814–825.
Wang, J., Jiang, M., Lu, F., 1998. J. Electroanal. Chem. 444, 127–132.
Wang, X., Zhi, L.J., Mullen, K., 2008. Nano Lett., 323–327.
Wang, Z., Wang, H., Zhang, Z., Liu, G., 2014. Sens. Actuators, B 199, 7–14.
Wang, Y.C., Cokeliler, D., Gunasekaran, S., 2015. Electroanalysis 27, 2527–2536.
Windmiller, J.R., Wang, J., 2013. Electroanalysis 2, 29–46.
Wisitsoraat, A., Pakapongpan, S., Sriprachuabwong, C., Phokharatkul, D., Sritongkham, P., Lomas, T., Tuantranont, A., 2013. J. Electroanal. Chem. 704, 208–213.
Wu, Y., Xue, P., Kang, Y., Hui, K.M., 2013. Anal. Chem. 85, 8661–8668.
Xin, Y., Fu-bing, X., Hong-wei, L., Feng, W., Di-zhao, C., Zhao-yang, W., 2013. Electrochim. Acta 109, 750–755.
Xue, C., Kung, C.-C., Gao, M., Liu, C.-C., Dai, L., Urbas, A., Li, Q., 2015. Sens. Bio-Sens. Res. 3, 7–11.
Yang, J., Yu, J.H., Strickler, J.R., Chang, W.J., Gunasekaran, S., 2013. Biosens. Bioelectron. 47, 530–538.
Yang, S.B., Feng, X.L., Ivanovici, S., Mullen, K., 2010. Angew. Chem. Int. Ed. 49, 8408–8411.
Yang, X., Wu, F., Chen, D.-Z., Lin, H.-W., 2014. Sens. Actuators, B 192, 529–535.
Zhao, G., Li, J., Ren, X., Chen, C., Wang, X., 2011. Environ. Sci. Technol. 45, 10454–10462.
Zhu, Z., Garcia-Gancedo, L., Flewitt, A.J., Xie, H., Moussy, F., Milne, W.I., 2012. Sensors 12, 5996–6022.